CHAPTER 3

CLIMATE MODELLING ON REGIONAL SPATIAL SCALES

3.1 INTRODUCTION

In an effort to improve our understudying of the many aspects that govern atmospheric circulation, scientists expressed the flow in the atmosphere in terms of the primitive equations of flow dynamics (Rautenbach, 1999). At the end of the nineteenth century Bjerknes (1904) significantly contributed to the science of Numerical Weather Predictions (NWP). He was a pioneer by suggesting that, given prescribed observed initial fields, it was possible to determine the prognoses of atmospheric flow at any future time by numerically solving the hydro-dynamical equations. In essence, NWP is an initial value problem since the accuracy of short-term forecasts rely upon the accuracy of the initial field used in the forecast simulation.

The British scientist Lewis Fry Richardson (1922) was the first to initiate routine weather prediction by means of numerical integration. Although his procedures were basically sound, there were some flows that resulted in large errors with respect to the observed fields. The enormous computing time required to solve the equations in the general form he used discouraged any immediate further attempts of NWP. However, theoretical research continued and led to some direct applications to practical problems. Caral-Gustaf Rossby (1939), for example, demonstrated the importance of linearized perturbation of the equations of motion in NWP (Haltiner and Williams, 1980).

It was another invention in the late 1940s, namely the electronic computer that led to a new breakthrough. This enabled Charney *et al*. (1950) to produce the first successful NWP in 1951 where after he wrote a scientific paper about anticipated future development in the discipline of NWP. Following this development, Lorenz (1963) proposed that prediction of the atmospheric state was not possible, unless present atmospheric conditions were precisely known. Owing to the inevitable

inaccuracy and incompleteness of weather observation in some areas of the globe, it is still not possible to produce the ideal initial field. Lorenz also discovered that the chaotic (or non-linear) nature of the atmosphere imposed a finite limit of about two weeks to NWP. At that time his fundamental discovery was "only of academic interest" and not actually relevant to operational NWP since the accuracy of even a 2-day forecast was rather poor. Since these discoveries computer-based NWPs have improved to such an extent that Lorenz's limit of predictability started to became nearly attainable in practice, especially with ensemble forecasting. Scientists also start to explore the predictability of longer-range atmospheric propagation, such as predictions of the El Niño (Kalnay *et al*., 1998) or simulations of the Earth's climate. These efforts, however, required energy conservation in the formulation of the atmospheric equations (Haltiner and Williams, 1980).

Climate modelling is young but fast developing science. Both ocean and land surface processes as simulated by climate models had developed from simple specified surfaces to highly parameterised processes in present GCM codes. According to Henderson-Seller and McGuffeie (2001) the development of computational power and the capability for forecast have been exponential. The computational capability currently available still lags behind, and to a large extend inhibits the resolution of GCMs to resolve local or regional scale process. Nested Climate Models (NCMs) were introduced to achieve regional climate simulations. GCMs and NCMs have reached a high level of sophistication. GCMs are currently widely employed to produce climate simulations on a global scale, while NCMs are nested within these models to produce more detailed regional simulations.

This chapter explores the fundamentals of atmospheric modelling by putting particular emphasis on NCMs and their capabilities. It also highlights the ultimate reasons that led to the formulation of NCMs, and how NCMs simulations added value to GCMs results.

3.2 GLOBAL GENERAL CIRCULATION MODELS

The fundamental process driving the global climate system is heating by incoming short-wave solar radiation and the subsequent cooling by outgoing long-wave infrared radiation into space (Cubasch and Cess, 1990). This heat flux exchange keeps the global temperature of the Earth close to constant, and to a

great extend modulate the global atmospheric circulation, which in turn, influences complex smaller scale flow patterns found in the atmosphere. A climate model simulation is therefore an attempt to simulate these complex atmospheric processes that govern Earth's climate. Many aspects of the climate are not yet well understood, and a significant number of the uncertainties when modelling the atmosphere, ocean and cryosphere are still directly related to the lack or knowledge (Henderson-Seller and McGuffeie, 1987). GCM simulations therefore strive to calculate the full three-dimensional character of the climate comprising at least the global atmosphere and the oceans (Henderson-Seller and McGuffeie, 2001). In GCMs the major Earth system components that affects climate are normally represented in sub-models (atmosphere, ocean, land surface, crysosphere and biosphere), accompanied by specific physical formulations that link these components in order to produce a balanced climate simulation (IPCC WGI, 2001).

GCM dynamics are represented by the governing atmospheric equation that include the equation of motion (Newton's second law), the first law of thermodynamics, the law of conservation of mass or continuity equation, the equation of state (ideal gas law) and the conservation equation of the water substances such as moisture (Haltiner, 1971). Those processes not explicitly governed by the atmospheric equations in the model dynamics are integrated into the model by means of physical parameterisations (see section 3.7).

3.3 THE NEED FOR DOWN-SCALING

On the synoptic scale, present global GCMs succeed to adequately simulate the main characteristics of the atmospheric circulation (Engelbrect *et al.,* 2002). However, most GCMs employed for climate variability and climate change studies have a coarse resolution owing to computational requirements (McGregor, 1993). Finer grid resolutions require smaller time steps that lead to more numerical equations to solve for a specific simulation to be completed.

For this reason, most current GCMs do not have a resolution fine enough to resolve meso-scale processes, which are often necessary for local or regional scale impact assessment modelling. As an alternative regional NCMs were introduced to obtain more detailed climate simulations for selected regions on the globe. These models are nested within global GCMs, and are fed across its lateral

boundaries by information produced by the GCM. It should, however, be emphasised that NCMs are not formulated to replace GCMs, but rather to supplement GCMs by adding downscaled detail to the coarser resolution of GCMs (Jones *et al.,* 2003).

3.4 DOWNSCALING APPROACH

The essence of climate modelling is to produce applicable detailed (high-resolution) atmospheric pattern data over the largest-possible area for the longest period of time. Observational data introduced through a process of data assimilation yields improved initial conditions, and reliable boundary conditions such as topography and surface energy forcing (vegetation, soil type and ocean temperatures) ensures that the model (either a GCM or NCM) receives adequate information across its boundaries. Vegetation forcing, land-water contrast urban effects (heat islands) may cause significant climate signals such as topographical precipitation, sea breezes and lake and heat island circulation. To include all these detail on a global fine resolution grid demands a high level of computational capability. The process of downscaling, where simulated results from a GCM is fed into either a NCM or statistical package, becomes an attractive alternative to produce detailed results over an area of interest.

When NCM research started in the late 1980s, GCMs had a horizontal grid resolution of approximately 300-500 km. These models were not suitable for regional or local scale climate change or climate variability studies. The process of downscaling was introduced and both statistical and dynamical models were developed for this purpose (Leung *et al.*, 2003). These two basic methods of downscaling may also be combined into a hybrid downscaling process if used simultaneously. Downscaling is a process of refining GCM output spatially and/or temporally to produce more detailed information on a local or regional scale.

3.5 NESTED CLIMATE MODELS

In resent years, much attention has been given to the understanding of climate variability on the sub-continental or regional spatial scales. This was mostly done through the application of NCMs or other Regional Climate Models (RCMs) (Engelbrect *et al.,* 2002; McGregor *et al*., 1993). The nested climate modelling approach allows for a finer resolution model (defined over a limited area) to be

nested within simulations results produced by a GCM. More detailed simulations are produced over the region of interest, which includes detailed topography, vegetation types, soil types and smaller scale meteorological phenomenon that might occur in the NCM domain. NCMs are therefore sound alternatives for performing high-resolution climate simulations over any area of interest on the globe.

During model simulations information is supplied by the GCM that is fed across the lateral boundaries of the NCM. When GCM fields are interpolated in time and space to fit the NCM resolution on its boundaries, a buffer zone is introduced over the boundaries of the NCM domain. This allow for a smooth transfer of information across the boundaries. Four and eight NCM grid points, starting from the boundary towards the centre of the NCM domain, are usually considered for the buffer zone.

No matter which type of nesting procedure is employed, it seems to be important to account for consistency between the model physics of the GCM and NCM as the model resolution gets finer. When the model resolution becomes fine enough to resolve processes such as convection, the convection parameterisation needs to be excluded from the NCM. It is, however, still an unresolved problem to diagnose the exact border where the parameterisation physics needs to be withdrawn (Leung *et al.*, 2003).

3.5.1 TYPES OF NESTING

3.5.1.1 ONE-WAY NESTING

Nested climate modelling requires that boundary information propagate from the GCM into the NCM domain. One-way nesting only permits disturbances in the coarse grid to enter the fine grid of the NCM while tow-way nesting (see next section) allows disturbances to enter and leave the fine nested grid mesh. However, many NCMs developed to date employ the so-called "relaxation" method to generate meteorological lateral boundary conditions for one-way nesting (Engelbrecht, 2000). The purpose is to force the NCM resolution towards the coarser resolution field over a lateral boundary zone. An alternative one-way nesting technique is spectral nesting. In this scheme, the GCM forces the low

wavenumber component of fields in the regional domain while the NCM calculates the high wavenumber components (Houghton *et al.,* 1995).

One-way nesting, as explained by McGregor *et al.* (1993), is a widely used approach where the flow of information occurs only from the GCM grid to the NCM grid. Nested modelling requires that boundary information to propagate freely into the nested domain and that the nested model does not suffer excessive reflection of its generated flows. A commonly used scheme is that of the relaxation method first suggested by Davies (1976). In this scheme, several (typically five) boundary rows form a buffer zone at each time step with full incorporation of the outer solution at the outermost rows, tapering off over the inner rows to the internal solution of the NCM. A slightly different one-way nesting scheme is that of Perkely and Kreizberg (1974). In this scheme there are four buffer rows over which the tendencies of the models variables are weighted. In a three-dimensional atmospheric model, the disturbances are more complicated and travel from many directions, so full attenuation of the reflections is not achieved. The residual reflections are mainly manifested near the horizontal boundaries in the divergence field, which may lead to some noise in vertical velocity and related precipitation patterns. Although the precipitation patterns may appear somewhat noisy near the boundaries, it should be noted that this noise does not ordinarily lead to contamination of the interior fields. This is because the GCM moisture and temperature fields strongly override the modifications made to the heating and drying of the NCM in the boundary zone.

3.5.1.2 TWO-WAY NESTING

In one-way nesting approach the circulation produced by the NCM does not feed back into the GCM (Engelbrect, 2000). It would be most appropriate if boundary information could propagate freely into and out of the NCM (two-way flow of information). This is actually more difficult to achieve than one-way nesting if the GCM and NCM have different architectures (McGregor, *et al*. 1997). Norris and Doty (1998) have reported the inclusion of two-way nesting scheme in MM5 nested regional model.

3.5.2.3 MULTIPLE NESTING

Multiple nesting is similar to one-way nesting, where one NCM is forced at its lateral boundaries by a second coarser resolution NCM, instead of by GCM. This approach is applied to yield high-resolution meteorological fields to capture small-scale processes such as thunderstorms.

3.6 NUMERICAL INTEGRATION OF CLIMATE MODELS

The formulation of atmospheric dynamics, parameterisation schemes and numerical integration techniques applied in both NCMs and GCMs are essentially similar. The major difference is that a NCM covers a limited area within a global GCM, and that atmospheric mass and temperature fluxes continuously crossing the boundaries of the NCM domain. As the NCM does not consider any atmospheric circulation features outside its domain, it needs to receive far field global information across its boundaries.

For large-scale atmospheric motion, the atmosphere is normally assumed to be in hydrostatic equilibrium, i.e., the vertical acceleration may be neglected (Haltiner, 1971). This assumption, known as the hydrostatic assumption, is currently widely applied in climate GCMs. The hydrostatic approximation is found to be valid for grid resolutions greater than approximately 10km. Inaccuracies may arise over steep terrain or during deep convention when finer grid resolutions are considered (McGregor *et al.,* 1993).

Generally, the accuracy of global weather and climate GCMs depends on many factors, including the accuracy of the knowledge of the state of the atmosphere at the initial time of model simulation, the numerical methods applied, and the horizontal grid and vertical layer resolution (Layton, 2003). Most GCMs use a sigma or hybrid- sigma vertical coordinate which is terrain following at the surface of the Earth, while the upper air coordinate gradually changes to follow a surface of constant pressure or potential temperature. On the horizontal plane most global GCMs consider a spherical coordinate that follows longitudes and latitude to solve the advection equations. A well-known disadvantage of spherical coordinates is the convergence of the meridians of the latitude-longitude grid toward the poles. This is often controlled by the use of Fourier filtering along latitude lines for grid point models to avoid time step restrictions (McGregor, 1995 b). However, for computational reasons, accuracy and uniform applicability of physical parameterisation more uniform regular horizontal grids are used in

NCMs. For example, the Lambert Conformal, Gnomonic Cubic (Sadourny, 1972) and Conformal Cubic coordinates (Rančić *et al.,* 1995) may be mentioned. The latter is engaged in stretch grid models (McGregor, 1995a). It implies that the horizontal grid projection of a global GCM does not always fit the projection of the NCM grid. This might give rise to interpolation instabilities at the lateral boundaries of NCMs.

As detailed by Layton (2003), GCM and NCM integrations require calculations that are known to be very time-consuming on even modern computers. In particular, a long-standing problem in the integration of NWP models is related to Eulerian time discretization where the maximum permissible time step is restricted by stability rather than accuracy. This implied that for an integration to be stable, the time step has to be small enough for the time truncation error to be much smaller than the spatial truncation error. Smaller time steps obviously require more computer time. Early models used an explicit Leapfrog method in numerical integration, where the time step was limited by both the Courant–Friedrichs–Lewy (CFL) criteria and propagation of gravity waves. Discretization schemes based upon the semi-Lagrangian treatment of advection offer the promise of larger time steps, with relatively no loss in accuracy compared to Eulerian-based advection schemes (Robert, 1981; Staniforth & Côté, 1991). Since gravity terms may render the equations stiff and thus severely restrict the time step (even with semi-Lagrangian advection approximations) one needs to combine the semi-Lagrangian formulation with semi-implicit time-stepping to obtain maximum benefit from the semi-Lagrangian approach. By combining a semi-Lagrangian treatment of advection and a semi-implicit treatment of gravity terms, it is possible to increase the time step substantially while maintaining numerical stability.

3.7 PHYSICAL PARAMETERISATION IN CLIMATE MODELS

Because of their large grid-box dimension, global climate GCMs do not explicitly represent small-scale process occurring within the atmosphere-surface-ocean continuum. In order to produce realistic simulations (Kalnay *et al.,* 1998), a climate model needs to have an accurate representation of the net effect of small-scale physical processes in the climate system. These processes proved to be important for model performance. Physical parameterisation is the representations of those processes in a model that are not explicitly governed by the dynamic atmospheric equations (Hewitson, 2001). The most important fields

of physical parameterisation include the radiation balance, clouds and precipitation processes (dynamic and convective), boundary layer processes, surface and sub-surface processes atmospheric chemistry and gravity wave drag.

As noted before, the primary factor that drives atmosphere circulation is the differential solar radiation between the poles and the equator and the subsequent radiation budget that needs to be in balance. The processes involved in the radiation budget are very complex and too time consuming to compute for numerical prediction purposes (Fu *et al*., 1995). Hence simplified radiation schemes are used in atmospheric models (e.g., Katayama, 1974 see Haltiner and Williams, 1980). These simplifications and stochastic approximations of physical processes in the atmosphere are typical examples of physical parameterisation.

Cumulus convection plays a major role in the vertical transport of heat and moisture in the atmosphere. Cumulus parameterisation has been a topic of considerable interest since the first studies by Charney and Eliassen (1964) and Ooyama (1964) who focused on the growth of tropical cyclones. Following this development, many cumulus convection parameterisation schemes have been developed for atmospheric models. These vary from rather simplistic moist convective adjustment schemes (Kuo, 1974) to sophisticated approaches, which include more detailed cloud physics (Arakawa and Schubert, 1974; Anthes, 1977). While individual clouds might not be resolved in large-scale atmospheric models, a collection of these clouds may have an important impact on the large-scale heat and moisture budget of the atmosphere. Consequently, it is necessary to parameterise the effects of cumulus clouds as a function of the large-scale fields of temperature, moisture, and momentum (Albrecht, 1983).

Since cloud formation and rainfall are important for sustainable live on Earth, many parameterisation schemes representing cloud and precipitation processes have been developed over the last few decades to allow for more realistic simulations in global GCMs and NCMs. Cloud and rainfall parameterisation is linked to dynamic related atmospheric properties such as temperature, humidity and wind velocities at a specific time-step. Such parameterisation schemes, which are applied to “correct” the atmosphere at given time steps, are known as diagnostic schemes and are widely used in large-scale models (Slingo, 1987). Sophisticated prognostic schemes have also been developed to reflect microphysical processes in clouds and the interaction of cloud processes with the

surrounding atmosphere (Sundquist, 1978; Smith, 1990). Nevertheless, all these processes are still an oversimplification of real atmosphere-cloud processes.

2.8 MODEL SIMULATIONS ON LONGER TIME-SCALES

Weather refers to the day-to-day state of the atmosphere. It describes the formation and propagation of fronts and individual storms, daily precipitation, temperature, humidity, winds and Mean Sea Level Pressure (MSLP) patterns. While great progress has been made in the field of forecasts on longer time scales, the chaotic behaviour of the atmosphere hinders the predictability of day-to-day weather fluctuation beyond Lorenz's limit and there is no scientific basis for forecasting beyond this limit (AMS, 2001). Apart from the impact of chaos, accurate observations of the initial atmospheric state (initial conditions) are crucial for short-term weather forecasting.

In longer-term forecasts and simulations (seasonal and climate) initial conditions do have a detectable influence at the initial phase of the simulation, although they become less important as the simulation progresses in time. Here boundary forcing plays an important role in keeping the model simulation on track and prevents it from drifting. When boundary forcing such as fluxes from the upper ocean, ice sheets or land surface are coupled to the atmosphere and are allowed to evolve, longer time-scale model simulations may be achieved (Goddard *et al.,* 2001). Boundary forcing from changing Sea Surface Temperatures (SSTs) makes seasonal forecasting possible, while climate change scenarios may be produced when a model is forced with changing concentrations of greenhouse gasses. It is obviously also important that energy is conserved in the formulation of the atmospheric equations of climate simulations.

CHPATER 4

CHARACTERISTICS OF THE PAST AND PRESENT CLIMATE OF ERITREA

4.1 INTRODUCTION

Historical data for large parts of Africa either does not exists or is not regarded as reliable. At present regional-scale observational records of temperature and rainfall are limited, and there is little prospect of reconstructing temperature and rainfall records from historical data alone unless more knowledge of paleoclimatology in Africa is gained. It is therefore sound to include proxy data from other sources, such as tree growth indices, ice-cores and sedimentary deposits along with historical data for paleocliamte reconstruction over the past few centuries (Bradley, 1991). Despite the uncertainty in historical records, many researchers have searched for evidences of more extreme fluctuations in temperature over the past 500 years than observed since the industrial revolution that started in 1860 (Nicholson, 1979; MacCracken and Kutzbach, 1991).

Studies of past climates are useful in identifying mechanisms and processes that might have led to large changes in climate. These studies might also contribute to climate model verification and improvement (MacCracken and Kutzbach, 1991). However, such information is of little value in current social infrastructure and natural resource management activities.

A widely used and easily available observational datasets for more recent model comparison are the global reanalysis data set from the National Center for Environmental Prediction (NCEP) (Kalnay *et al*., 1996) and European Centre for Medium-Range Weather Forecasts (ECMWF) (Gibson *et al*., 1997). NCEP data is available for many variables since the mid-1970s, and it covers the African continent with a horizontal resolution of 2.5^{o} x 2.5^{o}. Some variables are also available on horizontal levels in the vertical. Although not particularly ideal for local or regional scale model verification (because of its coarse resolution), the NCEP reanalysis is most probably among the best data set presently available for this purpose.

In Eritrea there are a number of meteorological stations distributed all over the country. Observed data from most of these stations appear to be unreliable owing to a lack of continuity and standardization. Nonetheless, attempts are under way to incorporate some of the locally observed rainfall data to supplement NCEP reanalysis data in order to investigate past and present climate trends over Eritrea.

This chapter gives an introduction on how past climates evolved in the sub-Saharan Africa and Eritrea region. It also gives detail about the characteristics of the present Eritrea climate, and explores previous views on the driving mechanisms of atmospheric circulation and of persistent droughts that became more frequent over the past two decades.

4.2 OBSERVED CLIMATE PATTERNS

4.2.1 ATMOSPHERIC CIRCULATION

Describing characteristics of the present atmospheric general circulation provide an appropriate starting point for elaborating on the climate of Eritrea. Larger scale atmospheric circulation plays an important role in the occurrence of wet and dry spells in the region. Characteristics of global atmospheric circulation for January and July are well documented in the literature (Ahrens, 2000; Martyn, 1992; Nicholson and Flohn, 1980). Although it is beyond the scope of this chapter to provide detail of the global atmospheric circulation, it is worthwhile to firstly give an overview of the global circulation that affects Eritrea before addressing local climate properties, which extend from the climate of Eritrea to the climate in small-scale river basin catchments.

4.2.1.1 MEAN SEA LEVEL PRESSURE AND NEAR-SURFACE WIND PATTERNS

In reality there are a number of latitudinal synoptic-scale bands of alternating low and high-pressure systems that propagate in the atmosphere with their associated wind flow patterns. In the equatorial zone, a semi-stationary band of low-pressure systems occur on average. Due to solar heating and strong convection, a region of thunderstorms and frequent rain developed that is referred to as the Inter-Tropical

Convergence Zone (ITCZ). North and south of the ITCZ (at approximately 30^{o} latitude), subtropical anticyclones occur which are associated with descending air masses that result in drier conditions. Further pole wards, mid-latitudes cyclones and high-pressure areas of the circumpolar regions are found.

Important for Eritrean climate are the Northern Hemisphere subtropical Bermuda-Azores anticyclone positioned over the eastern Atlantic Ocean (between 25^{o}N and 35^{o}N) and the Pacific anticyclone – both systems occur throughout the year. These two anticyclones developed in response to the convergence of air aloft near the upper-level jet stream that forms part of the well-known Hadley cell. Two wind patterns, namely prevailing westerlies to the north of these systems and easterly trade winds to the south are a result of the angular momentum balance of the planet's atmosphere. Easterly trade winds form a significant part of onshore mass flux over northeastern Africa. However, during May to September (spring season) the central Asian high-pressure cell decays to form a shallow Pakistani thermal low in association with the ITCZ. During winter (October to April), owing to the intense cooling of the Asian continent, a high-pressure cell develops over Asia to interact with the other Northern Hemisphere subtropical anticyclones. In the southern hemisphere, three clearly defined subtropical anticyclones appear over the three oceans that are separated by southern Africa, South America and Australia.

Synoptic-scale atmospheric circulation cells associated with subsidence and convection of air over specific regions have recently attracted a lot of interest, especially with respect to drought patterns (see section 4.4). In the tropics atmospheric circulation is governed to a great extend by Hadley cell circulation that is associated with convection over the ITCZ and subsidence over the subtropics. Subsidence in the subtropics is most pronounced over the oceans (Nicholson and Flohn, 1980). During the northward migration of the ITCZ in Boreal summer months (June-July-August (JJA)), convection accompanied by local forcing plays an important role in the weather of the Eritrea region. The northward migration of the ITCZ towards the Sahara is accompanied by the west African monsoon, which allows for air flow from the west over the northern African continent. Winds from the African monsoon often reach Eritrea from the west.

The central east African highland meandered across a north-south alignment (east of the Nile valley). Its northern boundary is located in Eritrea and its

southern boundary over central-east Africa. This highland, the Red Sea, the Gulf of Aden, the Gulf of Guinea and the high altitude Asian landmass all contribute noticeably to the weather of Eritrea by affecting the movement of air masses with dry or wet attributes depending on the origin of flow and route followed.

The near-surface wind and MSLP climate as illustrated in figure 4.1 (a), (b), (c) and (d) demonstrate the most important synoptic-scale atmospheric circulation features over Eritrea during the four Boreal seasons. The discussion, however, focuses on the JJA and December-January-February (DJF) seasons, owing to the similarity of these seasons to the remaining seasons (September-October-November (SON) and March-April-May (MAM)).

Boreal summer season (JJA)

The northward migration of the ITCZ marks the onset of the summer season in the Eritrea region, which happens in June. During the JJA season (Boreal summer season), counter-clockwise circulation around the Pakistani thermal low and clockwise rotation around the Bermuda high produce northerly winds that consists of cool and dry air. These winds propagate southwards from the Azores and Siberian highs before reaching the Eritrea region (figure 4.1(c)). The northerly winds confluence with West African monsoon flow from the southwest before flowing over Eritrea and the Red Sea region. The ITCZ forms where these two air masses “collide”. These wind patterns are referred to as *harmattan* over the Sahara and West Africa, and *Egyptian Current* in the northeast Africa section (Martyn, 1992).

The African monsoon flow originates from the Atlantic Ocean high-pressure system in the subtropics of the Southern Hemisphere. The flow propagates northwards across the equator where it turns eastwards as a result of the Coriolis force. When reaching the Gulf of Guinea, the flow therefore becomes westerly to southwesterly from where it advance across the Congo basin and Sahara towards northeast Africa. The unstable moist air in the African monsoon when reaching the African continent becomes drier as it flows over the African continent until it faced the dry and dust bearing of the Egyptian currents. The African monsoon persists during the May to September period (broader summer) with some minor changes in the MSLP fields and ITCZ location.

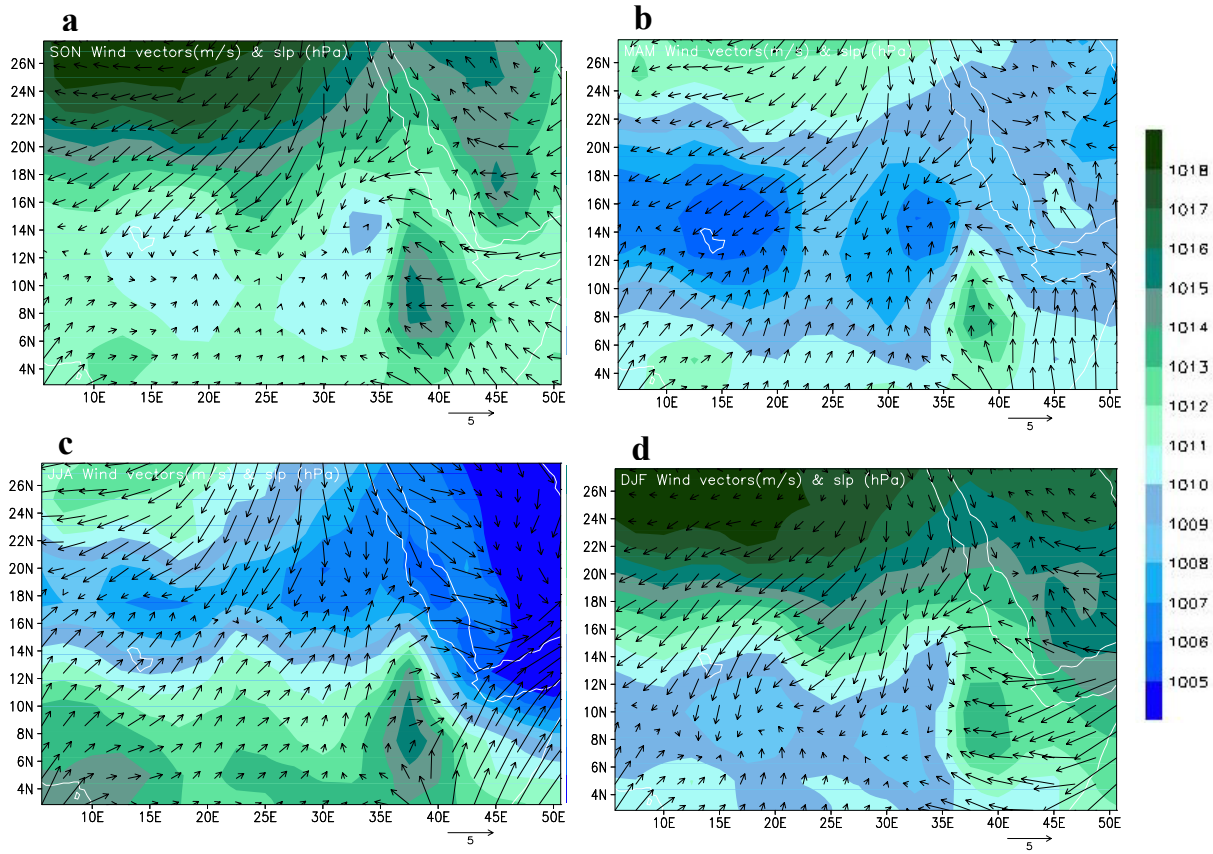

Figure 4.1: Observed seasonal Mean Sea Level Pressure (MSLP) in hPa and averaged near-surface winds (x10 ms^{-1}) over the period (1948-2003) as obtained from NCEP reanalysis data. The maps represent the four Boreal seasons namely, (a) September to November (SON), (b) March to May (MAM), (c) June to August (JJA) and (d) December to February (DJF).

Boreal winter season (FDJ)

During the Boreal winter season (DJF) the Asian continent cools down and the strong Siberian high-pressure system develops over central Asia. The clockwise rotation around this high result in intensified easterly trade winds towards Africa and a reverse in the Indian Monsoon flow. This allows for a strong easterly flow over the Red Sea and Eritrea (figure 4.1 (d)). The ITCZ migrates towards the south of the equator over east Africa, although it persists in the Northern Hemisphere over the west-African section.

Over the western parts of Eritrea, average winds flow parallel to the mountains of the central Highlands to move southwards to southwestwards. These winds contain little

moisture and allow for the prevalence of dry conditions over western Eritrea during DJF.

During the Boreal winter season circulation patterns are complex over the Red Sea region and the eastern escarpment of the Eritrea Highlands. Flow is predominantly from the east and southeast crossing the Red Sea before reaching Eritrea. Van Buskirk, *et al.* (1997) suggested the development of a cool humid inversion layer over the Red Sea ocean surface as a result of evaporation, with winds that is pushed to the west by synoptic gradients. These winds, under the influence of the central Highlands, "collide" with northerly flow from Egypt to form a small convergence zone. The former wind patterns are responsible for rainfall during the DJF season in the Red Sea and eastern escarpments of Eritrea, since moisture is imported form the Indian Ocean and Gulf of Eden.

4.2.1.2 MOISTURE ADVECTION AND RAINFALL PATTERNS

Tropical warm-season rainfall regimes are predominant on the African continent, although winter rains of extra-tropical origin prevail on its northern and southern extremes. Arid and semiarid zones, the Sahara and the Kalahari, mark the transition from tropical to extra-tropical influence. The primary control on rainfall in the tropical areas is the ITCZ, which advances northward to the Saharan margin in the Boreal summer and southward to the north of Kalahari in the Austral summer (Nicholson, 1986).

In Africa moisture flux becomes progressively less toward the north and south of the equator. It is evident that, even though the ITCZ's location is more northerly during the Boreal summer (JJA), the northward decrease of rainfall and moisture flux patterns seem to be not only controlled by the ITCZ, but also by the degree of convection, the availability of moisture and average synoptic forcing. Figure 4.2 (a), (b), (c) and (d) gives the daily precipitation, precipitable water, zonal and meridional moisture fluxes averaged over the season JJA and period 1948-2003. The climatology was calculated from the NCEP reanalysis data set. In general the moisture flux pattern are consistent with precipitation patterns (figure 4.2 (a), (b) and (c), (d)).

The west-Africa monsoon is responsible for substantial moisture flux from the Gulf of Guinea towards the ITCZ zone in Africa. Martyn (1992) linked these moisture

advection patterns to the general atmospheric circulation. The trade winds, blowing from the Atlantic high-pressure system in the Southern Hemisphere overwhelming consists of stable air. When crossing the equator while advecting northwards, the air becomes unstable due to the adherence of moisture. The resulting moisture transport is persisted until it meets the dry and dust bearing northeasterly and easterly Northern Hemisphere trade winds at ITCZ. The northward displacement of the ITCZ during JJA creates an opportunity for the African monsoon moisture to reach Eritrea, which also mark the beginning of the Boreal summer.

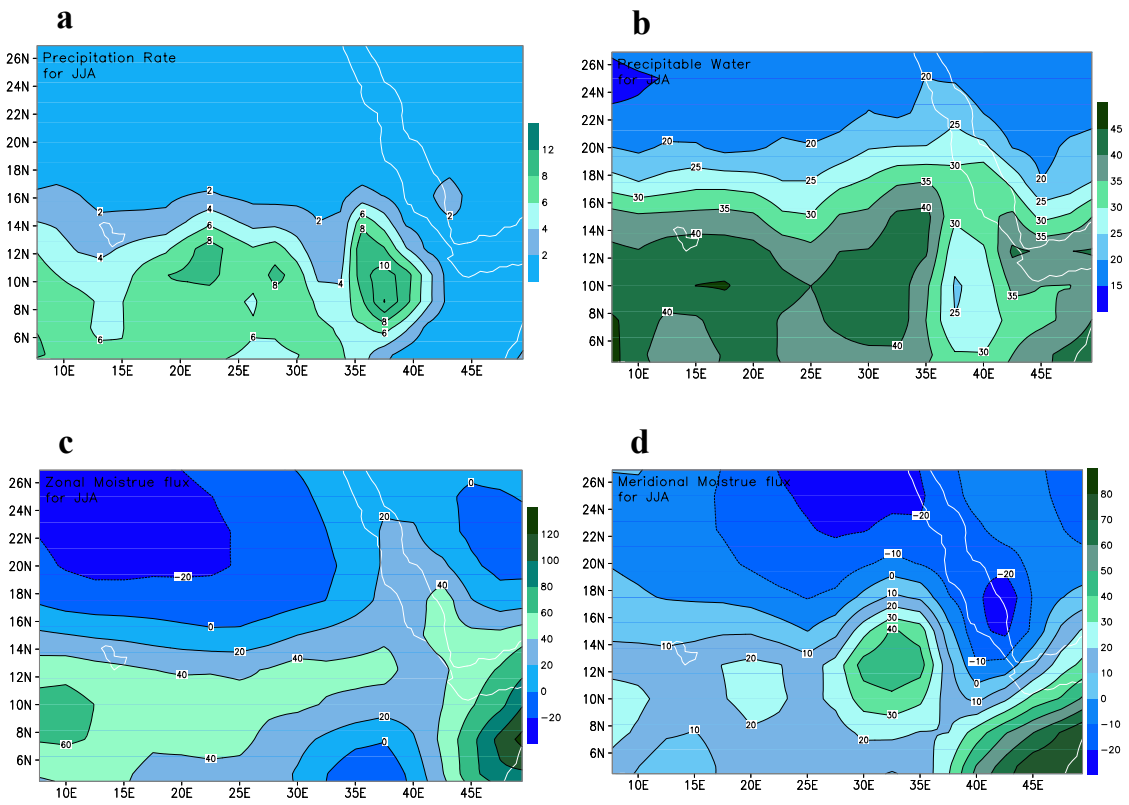

Figure 4.2: Observed (a) precipitation rate in mm per day, (b) precipitable water in kg m^{-2}, (c) zonal moisture flux and (d) meridional moisture flux in kg $m^{-1}s^{-1}$ averaged over the months June to August (JJA) and period 1948-2003. The climatology was calculated from the NCEP reanalysis data set.

Boreal summer season (JJA)

The driving mechanisms of Boreal summer rainfall over Eritrea are consistent with those that drive the Sahelian climate. It is mainly associated with tropical

circulation and constrained, to a large extend, by convective activities in the ITCZ. Over Eritrea rainfall extends from May to September, while reaching a peak during July and August. During this season the eastern Lowlands experience dry conditions. Martyn (1992) suggested this to be associated with the so-called foehn effect that appears on the lee side of mountains when air descends from a higher altitude. However, this is not affecting the eastern escarpments of Eritrea the eastern facing highlands are characterized by a bimodal (during JJA and DJF seasons) rainfall pattern as shown in figure 4.3. The higher rainfall along the eastern escarpment may be attributable to local influences such as evapotraspiration from a densely covered forest surface.

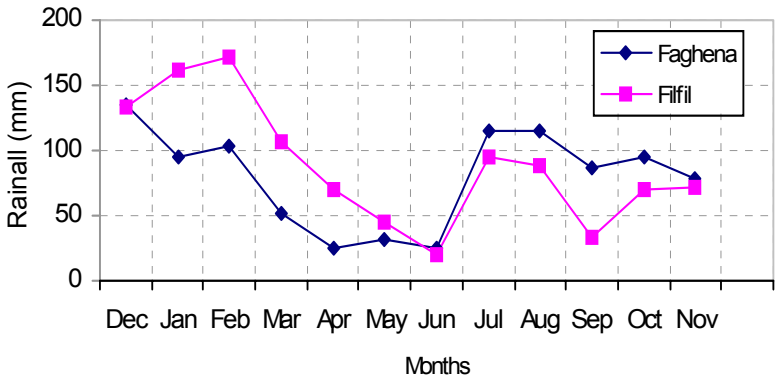

Figure 4.3: Observed mean monthly rainfall in mm for Filfil (1928-63) and Faghena (1947 to 1962) as obtained from the Department of Water Resources (DWR) of Eritrea. These two stations are found along the eastern escarpment of the Eritrea Highlands that is covered with remnants of the tropical rain forest and referred to as Green Belt.

Boreal winter season (DJF)

During DJF circulation and moisture advection patterns over Eritrea is not affected by tropical atmospheric systems since the ITCZ moves towards southern Africa in the eastern section of Africa. During the Boreal winter season winds bring moisture from northwestern Indian Ocean and Gulf of Eden. The moisture transport is responsible for rainfall in the Red Sea and along the eastern escarpment of the central Highland of Eritrea. On the Highland plateau and the western part of Eritrea, dry conditions prevail owing to the foehn effect.

4.3 OBSERVED CLIMATE TRENDS AND VARIABILITY

It has been well understood that climate variability, whether associated with internal or external climate system forcing, appears to modify the normal prevailed climate state of the atmosphere which in turn reinforce conditions that might lead to droughts or floods in different locations of the globe.

The Southern Oscillation (SO) is the best-defined and understood mode of international climate variability. Extreme phases of the SO are characterized by global-scale shifts in atmospheric circulation cells (normally Walker cells) and with a marked, high amplitude modulation of equatorial Pacific Ocean sea surface temperature anomalies (Ropelewski & Halpert, 1991) that include the formation of El Niño events. Currently, some percentage of interannual variability on the globe appears to be related to changes in tropical oceans temperatures associated with El Niño events. It is expected that greenhouse warming might equalize temperatures in the eastern and western Pacific Ocean by warming the cooler eastern Pacific Ocean. The heat of the warmer western Pacific is largely absorbed by increased evaporation. Such an expected decrease in El Niño events might obviously also reduce interannual variability on other parts of the globe (Rind, 1991).

The response of the climate over the northern east Africa region (Eritrea, Ethiopia, Somalia and Djibouti) to the SO and El Niño events is not well documented. Most studies focused on the western Sahle or central eastern Africa domain (Kenya, Tanzania, Uganda, Burundi and Rwanda). The climate behavior of the former region, especially over Eritrea and Ethiopia, shares some degree of similarity to that of the central eastern Africa region during periods when tropical circulation dominates. It was found that El Niño events are normally associated with positive rainfall anomalies over the entire eastern Africa region – with the exception of Sudan (Schreck and Fredrick, 2003).

In recent years observed increased temperatures that might be attributed to global warming might have already disturbed climate patterns over eastern Africa. With this in mind, Schreck and Fredrick (2003) studied climate variability over eastern Africa where they compared the recent climate to a longer-term climate. They concluded that the recent climate was associated with a rapidly intensifying global warming signal. They suggested that if the observed global warming trend

continues to intensify in coming decades, the climate and ENSO responses may be altered significantly over eastern Africa. The possible response of the future climate of this region under conditions of enhanced greenhouse gases concentrations will be discussed in more detail in chapters 5 and 6 of this document. This section will focus on observed trends and variability over the domain illustrated in figure 4.4, with specific emphasis on the Eritrea sub-domain (gray area).

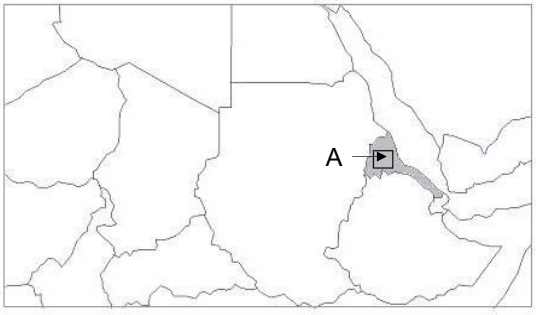

Figure 4.4: The domain that will be considered in PRECIS nested climate model (NCM) simulations. Eritrea is indicated in gray. In the following sections NCEP reanalysis data are spatially averaged over the box **A**.

4.3.1 RAINFALL

Trends and variability in rainfall is a matter of great importance, and a reliable long record of rainfall at different locations over the area of interest is essential when determining trends and investigating variance. Owing to many difficulties associated with rainfall measurement over Eritrea the use of station data alone is not recommended. For a country like Eritrea it is important to compare other moisture-related variables, such as stream flow and soil moisture with precipitation to generate a broader picture of long-term rainfall trends. Such analyses, however, are not addressed in this study.

As indicated in figure 4.5, the annual rainfall as recorded at Asmara (located on the central Highlands) shows a negative trend of approximately 0.87 mm.year^{-1}. During 1955-1960 and around 1980 anomalously high rainfall episodes were recorded in comparison to other decades. Prior to 1955 rainfall fluctuated around

the mean with a smaller variability. The dry episode during the last five years in the figure 4.5 was more severe than ever recoded since 1900.

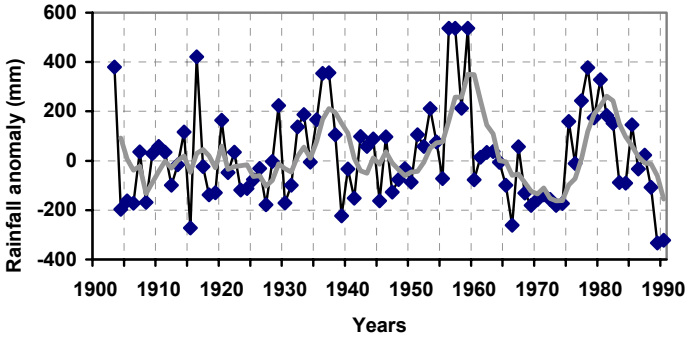

Figure 4.5: Annual rainfall anomalies (black line) and 5-years moving averages (gray line) over the period 1900-1990 for Asmara that is located on the central Highlands of Eritrea as obtained form the Department of Water Resources (DWR).

4.3.2 NEAR-SURFACE AIR TEMPERATURE

Variability of near-surface air temperatures calculated from NCEP reanalysis data over the period 1950 to 2000 for the four seasons DJF, MAM, JJA and SON were spatially averaged over both the entire domain of figure 4.4 and the box-area **A** in figure 4.4. Figures 4.6 (a), (b), (c) and (d) illustrate the weighted average time series of observed near-surface temperature anomalies (^{o}C) for the four seasons as calculated over the entire domain of figure 4.4. The gray lines represent five-year moving averages. Similarly, figures 4.7 (a), (b), (c) and (d) give the weighted average anomalies as calculated over the box-area **A**. According to these figures there are no obvious differences in air temperature variability over the two selected domains.

Figure 4.7 (a) shows a significant increasing trend in near-surface temperatures for the JJA season over the period 1948 to 1965. In contrast to an increase trend, it is interesting to note that temperature variability decreased over the same period. The general trends of near-surface temperatures during the SON and MAM seasons are similar to that of JJA, although higher variability appears in the SON and MAM time series. The trend of near-surface temperatures during DJF is not significant, but a warming episode appeared over the last decade.

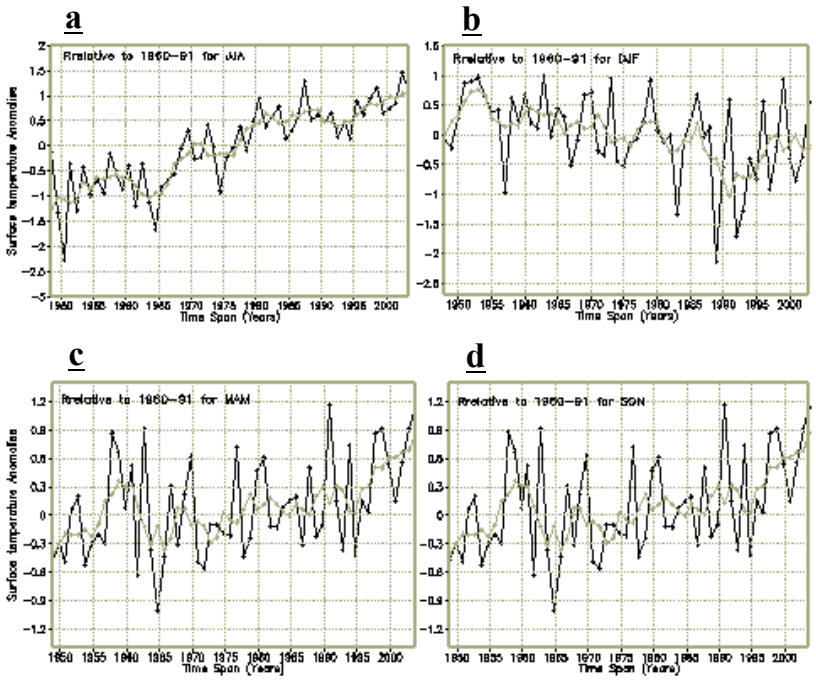

Figure 4.6: Weighted average time series (1950 to 2000) of near-surface temperature anomalies (°C) as calculated from NCEP reanalysis data for the seasons (a) JJA, (b) DJF, (c) MAM and (d) SON and the entire domain of figure 4.4. Gray lines denote five-year moving averages.

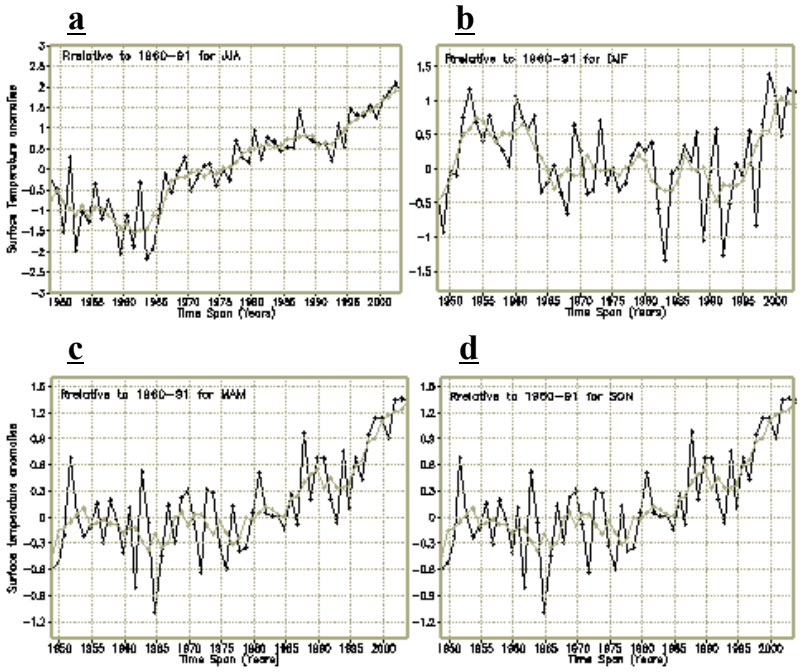

Figure 4.7: As figure 4.6 but averaged over box-area **A**.

4.3.3 MEAN SEA LEVEL PRESSURE

Variability of MSLP calculated from NCEP reanalysis data over the period 1950 to 2000 for the four seasons DJF, MAM, JJA and SON were spatially averaged over both the entire domain of figure 4.4 and the box-area **A** in figure 4.4. Figures 4.8 (a), (b), (c) and (d) illustrate the weighted average time series of observed MSLP anomalies (hPa) for the four seasons as calculated over the entire domain of figure 4.4. The gray lines represent five-year moving averages. Similarly, figures 4.9 (a), (b), (c) and (d) give the weighted average anomalies as calculated over the box-area **A**.

The MSLP during JJA (figure 4.9(a)) as well as in many of the other figures in 4.8 and 4.9 experienced a profound sink for the subsequent 10 years following 1954. It is interesting to compare this episode with rainfall in figure 4.5. During the same period Eritrea experienced persistent wet conditions. Higher rainfall is normally associated with a drop in MSLP since lower pressures is an indication of instability in the atmosphere. The MSLP anomalies do not show any significant trend, although it appears that MSLPs increased since the 1970s, but stabilized to a great extend thereafter.

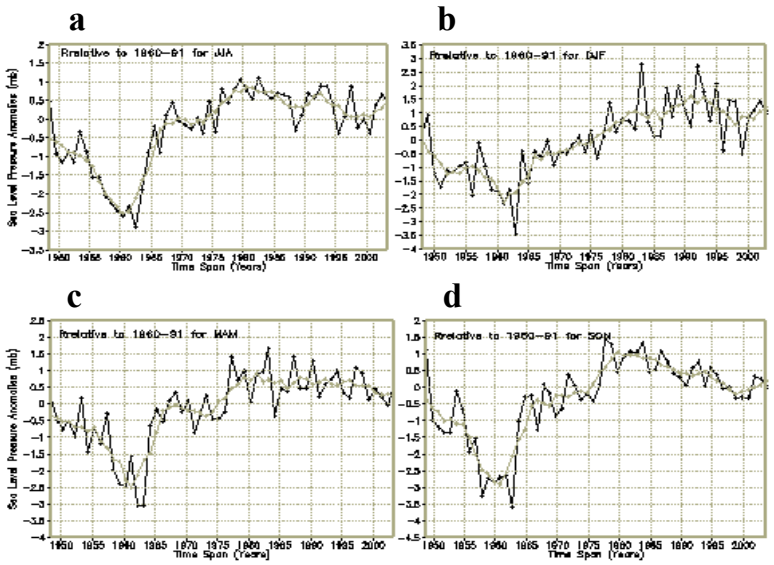

Figure 4.8: Weighted average time series (1950 to 2000) of Mean Sea Level Pressure (MSLP) anomalies (hPa) as calculated from NCEP reanalysis data for the seasons (a) JJA, (b) DJF, (c) MAM and (d) SON and the entire domain of figure 4.4. Gray lines denote five-year moving averages.

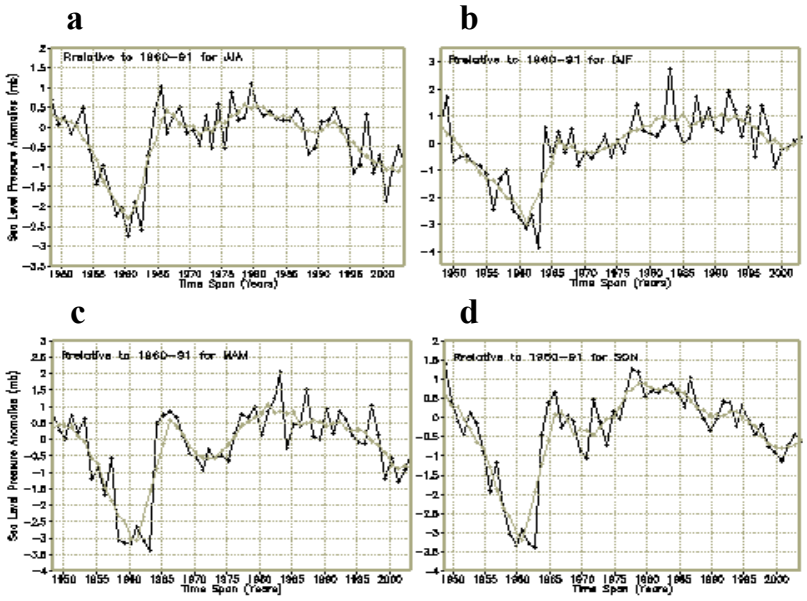

Figure 4.9: As figure 4.8 but averaged over box-area **A**.

4.4 DROUGHT EVENTS

Recent and present climate records of sub-Saharan Africa, and more particularly Eritrea, show frequent drought events that might be associated with the ENSO phenomenon. This section explores possible atmospheric mechanisms that might have led to these dry episodes.

4.4.1 BACKGROUND

There is strong evidence that the 16th and 18th centuries were generally wetter in the Soudano-Sahelian region than more recent decades, although drought episodes occurred in the 1680s and in the early to mid 18th century from 1738 to 1756 (Nicholson, 1981). Since then droughts became more frequent and more severe, particularly in the early 19th century (1800s to 1830s) and throughout the 20th century. In more recent decades trends pointed towards increasing arid conditions over large parts of Africa, which suggest that temperatures may have increased (Bradley, 1991).

The present climate of Sub-Saharan Africa is dominated by frequent drought events, which appear on the inter-annual and perhaps inter-decadal time scale. Drought is regarded a natural disaster that inflicts severe damage to ecosystems

and society in Africa. Despite many efforts to determine the driving mechanisms that cause droughts, scientists are still not sure whether more recent drought episodes evolve from natural forcing, such as ENSO, or from greenhouse warming.

4.4.2 PROPOSED DROUGHT MECHANISMS

Many researchers showed interest in the mechanisms that drove the persistent drought episodes that occurred in the Sahel-Sahara region over the last two decades. A general feeling is that these drought episodes might follow from a combined forcing from both natural and anthropogenic influences.

Charney (1975) attempted to relate the droughts in the Sahel region to biogeophysical feedback mechanism. According to his hypothesis the clearance of vegetation cover due to human activities, such as overgrazing, lead to an enhanced albedo. A higher albedo leads to a smaller fraction of radiation that is absorbed by the surface of the Earth, which in turn reduces heat and instability of the near-surface atmosphere. These conditions will result in higher pressures, increased subsidence and even dryer conditions. Walker and Rowntree (1977) emphasized the importance of soil moisture to the climate system and hypothesized that once the soil of a region gets wet, it produces a feedback to the atmosphere and biosphere for several weeks in advance. Nevertheless, initial sustained aridity and ground dryness alone could cause a desert to persist. As an extension of the research by Charney (1975), Cunnington and Rowntree (1986) indicated that any decrease in adiabatic heating, weather due to a reduced albedo or increased moisture availability, should lead to less instability and obviously less buoyancy. Rainfall will only appear if the lower atmosphere has enough energy to push the air upwards across the condensation level and higher. Reduced surface temperatures and adiabatic cooling might therefore lead to less rainfall.

Changes in synoptic and smaller scale atmospheric circulation patterns are also playing an important role in sustaining or suppressing conditions for persistent droughts. For example, the southward migration of the subsidence band of the Hadley cells in the subtropics promotes dry condition (Nicholson, 1886; 1991; Nicholson and Flohn, (1980). Nicholson (1983) suggested that the relative position of the ITCZ might modulate rainfall fluctuations (especially droughts). Similarly, Lamb (1978) and Foland *et al.* (1986) suggested that the gradual

infringement of the Saharan desert, which might be caused by regional or synoptic forcing, appears to be substantially influenced a southerly shift of the ITCZ. Owen and Folland (1988) indicated that global SST fluctuations were instrumental for initiating the humid 1950s and dry 1984s of the Sahel. Druyan and Hastenrath (1990) proposed that southward expansion of the mid-tropospheric jet might be the symptom of summer drought in the region.

CHAPTER 5

FUTURE CLIMATE PROJECTIONS FOR ERITREA FROM GCM SIMULATIONS

5.1 INTRODUCTION

A variety of paleoclimate, present and future simulations performed by GCMs intended to address the likelihood positive or negative trends in temperature and precipitation variability. At present there exists a general global inter-model consistency of possible changes as a result of greenhouse warming. Despite of an increase in global temperatures, diurnal temperature variability might likely decrease owing to a reduction in the latitudinal temperature gradient. Precipitation might increase owing to more evaporation (Mitchell, 1991; Rind, 1991). In some areas of the world the moisture content of the atmosphere might also increase without any noticeable changes in rainfall totals (Rind, 1991). The response of the general circulation of the atmosphere will obviously determine which areas might become drier and which areas might expect higher rainfall.

The objective of this chapter is to explore temperature and rainfall responses for the months January and July to model simulated climate change projections over the domain defined in figure 4.4, but with specific emphasis on the Eritrea sub-domain. Firstly results from greenhouse simulations from six GCMs used in the Inter-governmental Panel on Climate Change (IPCC) initiative will be analyzed in order to search for inter-model consistency signals in temperature and rainfall simulations. The A2 and B2 scenarios from the Special Report on Emission Scenarios (SRES) will be considered.

5.2 GLOBAL FUTURE CLIMATE CHANGE SIMULATIONS

The logic behind constructing future climate change simulations has been explained in depth in Chapter 9 of the report of the IPCC Working Group 1

(Cubasch, *et al*., 2001). It is worthwhile to briefly review the basics adopted in this report merely on the basis of contextual relevance and importance.

Studies on projections of possible future climate change use a hierarchy of coupled ocean/atmosphere/sea-ice/land surface models to provide indicators of global response as well as possible regional patterns of climate change. These types of more comprehensive fully coupled global climate models configuration was introduced in the late 1980s and are generally referred to as Atmosphere-Ocean Global Climate Models or Atmosphere-Ocean General Circulation Models (AOGCMs).

These highly sophisticated fully coupled GCMs evolved in such a way that models of the main components (atmosphere, land, ocean and sea ice) were mostly developed separately before they were gradually coupled. Most recently, sulphur cycle components have been incorporated to represent the emissions of sulphur and how they are oxidized to form aerosol particles. Currently in progress is the coupling of the land carbon cycle and ocean carbon cycle. The atmospheric chemistry component currently is modeled outside the climate model. The general trend in the evolution of GCMs development goes with notion of modeling of the Earth's climate system realistically so that all the components can interact and, thus, the predictions of climate change will continuously take into account the effect of feedbacks among components.

Despite these rapid developments in GCMs, it is yet hardly possible to produce accurate future climate change projections as a result of uncertainty. Reliable projections of future climate change as a result of increased greenhouse gas emissions could contribute significantly to early precaution actions, which might facilitate adaptation. Nevertheless, they are the only scientific resources currently available to produce some degree of guidance what might be expected in future climates.

Recently, the IPCC Working Group 1 released its third assessment report, and as part of this initiative prepared future climate change projections for Earth by introducing SRES greenhouse and aerosol forcing to AOGCMS. These SRES scenarios have been constructed to explore the future climate response to estimated greenhouse gas and aerosol precursor emissions. This response was simulated by using the only tool available for this purpose, namely GCMs.

The six GCMs used in the IPCC report are:

1. Canadian Centre for Climate modelling and analysis (CCCma)
2. UK Hadley Centre for climate prediction and Research (HadCM3)
3. Japanese Centre for climate system Research (NIES99)
4. Australian Commonwealth Scientific and Industrial Research Organization (CSIRO)
5. USA Geophysical Fluid Dynamics Laboratory (GFDL99)
6. German Climate Research Centre (ECHAM4)

5.3 GREENHOUSE GASSES AND AEROSOLS EMISSION SCENARIOS

GCMs are used to generate future climate change projections from prescribed atmospheric concentrations of greenhouse gasses and aerosols based upon specific emission scenarios. These forcing agents are the sole inputs to make a suite of projected future climate changes that illustrate the possibilities that might lie ahead.

In 1996, the IPCC began the development of a new set of emissions scenarios, effectively to update and replace the well Known IS92 scenarios (figure 5.1). Four different narrative storylines, which are illustrated below, were developed to describe the relationship between emission driving forces and their evolution and to add context for the scenario quantification as obtained from IPCC, WG1 (2001). The SRES scenarios do not include additional climate initiatives, which means that no scenarios are included that explicitly assuming implementation of the emissions targets of the Kyoto Protocol. However, greenhouse emissions are directly affected by non-climate change polices designed for a wide range of other purposes. Further more, government policies can, to varying degrees, influence the greenhouse gas emission drivers and this influence is broadly reflected in the storylines and resulting scenarios. In this chapter, as noted earlier, the six GCM projections that emanate from the A2 and B2 SRES scenarios are explored. The SRES scenarios are illustrated in figure 5.1.

The A1 SRES scenario describes a future world of very rapid economic growth, global population that peaks in mid-century and declines thereafter, and the rapid introduction of new and more efficient technologies. Major underlying the themes

are convergence among regions, capacity building and increased cultural and social interactions, with a substantial reduction in regional differences in per capita income. The A1 SRES scenario family develops into three groups that describe alternative directions of technological change in the energy system. The three A1 groups are distinguished by their technological emphasis: fossil intensive (A1F1), non-fossil energy sources (A1T), or a balance across all sources (A1B) (where balanced in defined as not relying too heavily on one particular energy source, on the assumption that similar improvements rates apply to all energy supply and end use technologies).

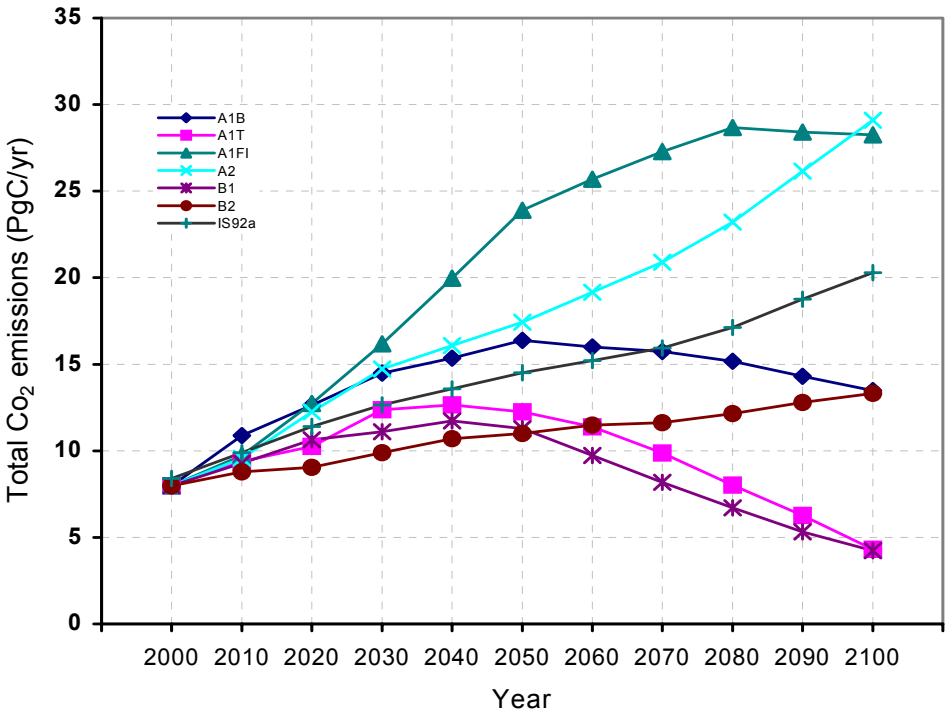

Figure 5.1: Anthropogenic emission projections of CO_2 for the six SRES scenarios, A1B, A2, B1 and B2, A1FI and A1T plus the updated and replaced well known the IS92a scenario as obtained from the IPCC Special Report on Emissions Scenarios (SRES) dataset (appendix II).

The A2 SRES scenario describes a very heterogeneous world. The Underlying them is self-reliance and preservation of local identities. Fertility patterns over regions converge very slowly, which results in continuously increasing population. Economic development is primarily regionally oriented and per capita economic

growth and technological change are more fragmented and slower than in other storylines.

The B1 SRES scenario describe a convergent world with the same global population, that peaks in mid-century and declines thereafter, as in the A2 storyline, but with rapid change in economic structures toward services and information economy, with reductions in material intensity and the introduction of clean and resource-efficient technologies. The emphasis is on global solutions to economic, social and environmental sustainability, including improved equity, but without additional climate initiatives.

The B2 SRES scenario describes a world in which the emphasis is on local solutions to economic, social and environmental sustainability. It is a world with continuously increasing global population, at a rate lower than A2, intermediate levels of economic development, and less rapid and more diverse technological change than in the B1 and A1 storylines. While the scenario is also oriented towards environmental protection and social equity, it focuses on local and regional levels.

5.4 IPCC GCM CLIMATE PROJECTIONS FOR ERITREA

IPCC GCM future climate projections of air temperature and precipitation rate (daily rainfall) relative to the base-line climatology (1961-1990) for January and July are investigated. The investigation explores projected changes for the 2080s with the A2 and B2 SRES scenarios. The domain under investigation is indicated in figure 4.4 with emphasis on the Eritrea sub-domain (shaded region in figure 4.4). The objective is to measure the aerial extent of the projected change and to explore if there exists inter-model consistency among the GCMs. High level of inter-model agreement gives an indication of the higher probability of the event to occur ahead and narrowing the range of uncertainty posed by both the natural randomness of the climate system and model physics (architecture) where the former uncertainty can only be quantified here.

The methodology followed to extract the statistical summaries of the projected climate changes from the Eritrea sub-region (denoted with letter “A” in the subsequent GCM maps) was done in two-steps. Firstly the coarse GCM boxes were replicated or regirded to finer grid boxes to suit the extraction along the

borders. Secondly the statistical summary was extracted from region "A" by masking out the remaining data. The scheme generates grid boxes based upon the original coarse grid box and broadcasts its value to the offsprings. In other words, the algorithm duplicates the coarse grid box into finer grid boxes with out sharing information from the adjacent grid boxes. For more information consult the "EXPAND" module in IDRISI software. The idea was to avoid additional uncertainty associated with interpolation. The GCM maps presented in the subsequent sections are, however, in their original resolution.

5.4.1 IPCC SIMULATED CLIMATE CHANGE SCENARIOS FOR JULY

5.4.1.1 AVERAGE NEAR-SURFACE TEMPERATURE PROJECTIONS

A2 and B2 SRES scenarios GCM projections of near-surface temperature for the 2080s as simulated by the six IPCC GCMs over the domain in figure 4.4 for July are illustrated in figures 5.2 and 5.3, respectively. Owing to the coarse resolution of the GCMs, no detail is available for Eritrea. However, averages of grid boxes that cover Eritrea were considered in the analysis that follows.

All the GCM projections showed above baseline near-surface temperature projections for 2080s for the whole domain with slight differences in the spatial distribution in both SRES scenarios. Accordingly, the HadCM3, CCCma, CSIRO, ECHAM4, GFDL99 and NIES99 GCMs project signals of near-surface temperature enhancement for the A2 and B2 SRES scenarios (figures 5.2 and 5.3). As shown in figure 5.4, there exists strong inter model consistency for near-surface temperatures among the GCMs. The NIES99 GCM simulated the smallest signal of A2 (+1.59 ^{o}C) and B2 (+0.92 ^{o}C).

The spatially averaged GCM near-surface temperature departures for Eritrea are in the order of +3.39 ^{o}C and +2.24 ^{o}C for the A2 and B2 SRES scenarios, respectively (figure 5.4(a)). The spatially averaged minimum (figure 5.4(b)) and maximum (figure 5.4(c)) values for Eritrea are in the range of +2.68^{o}C and +4.3^{o}C for the A2 SRES scenario, and +1.77^{o}C and +2.99^{o}C for the B2 SRES scenario. These two figures indicate the range of change fields in the considered sub-domain, i.e., figure 5.4(b) captures a grid box with the minimum value while figure 5.4(c) a grid box with the maximum value.

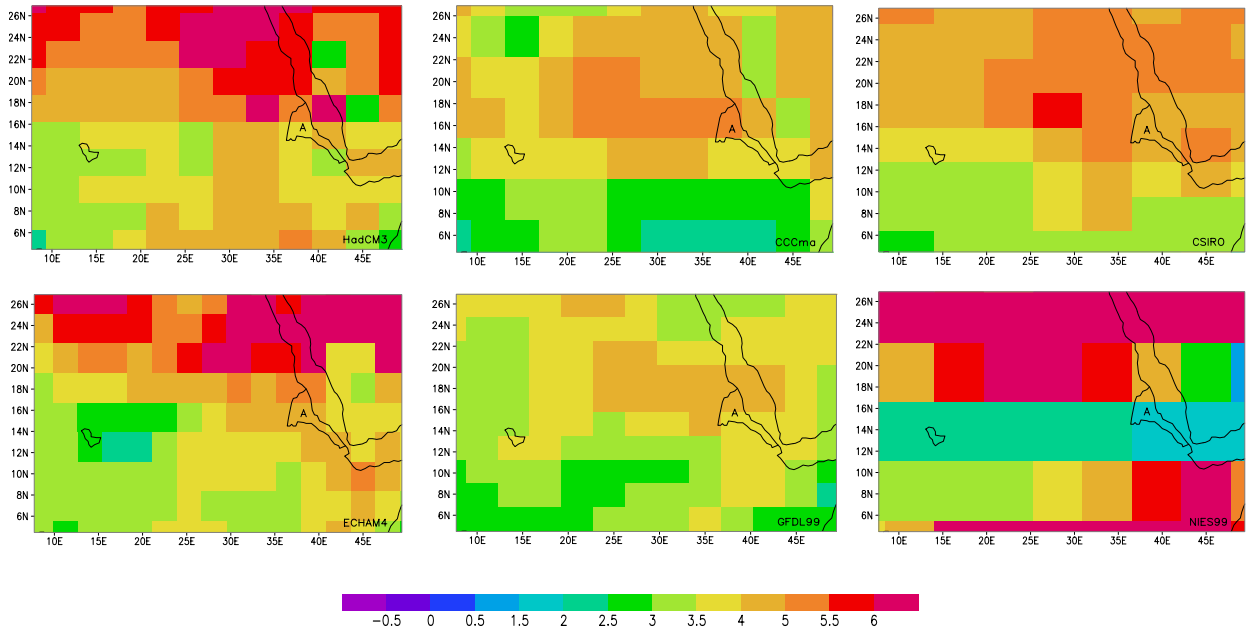

Figure 5.2: July near-surface temperature (°C) projections for the 2080s relative to 1961-90 for the six IPCC GCMs (indicated in the right bottom of each plot) for the A2 SRES scenario. Eritrea is indicated in letter "A".

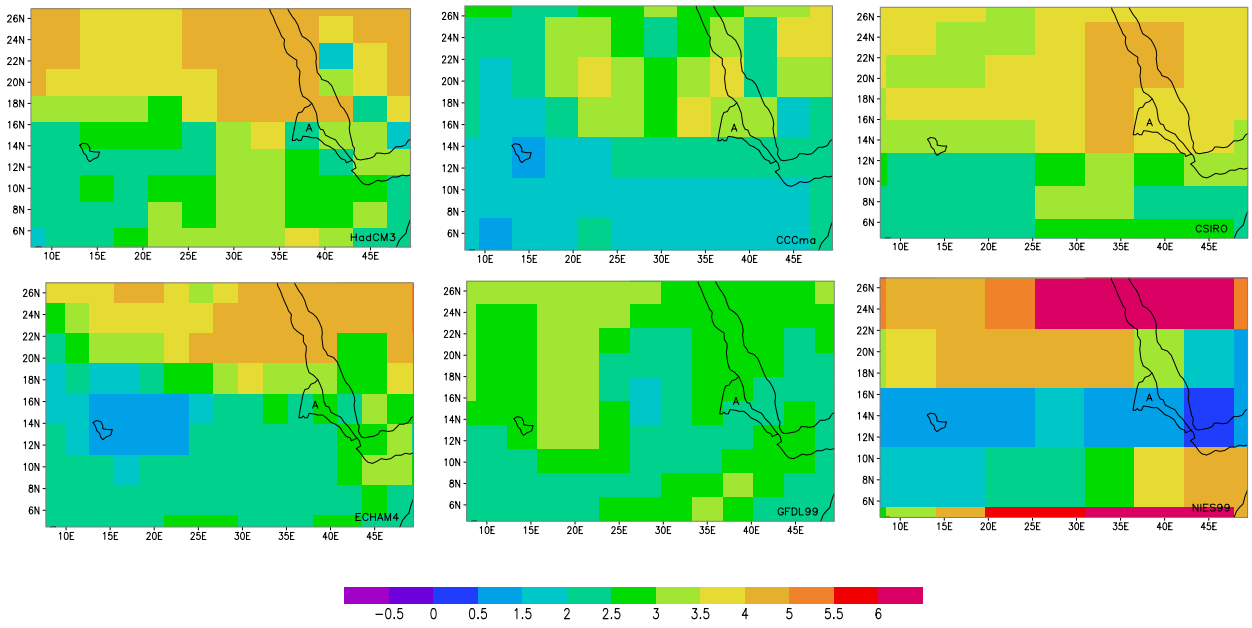

Figure 5.3: As figure 5.2 but for the B2 SRES scenario

This section indicates, according to the GCMs, that there exists a good possibility for warmer near-surface conditions during July in 2080s for Eritrea, with a 100% spatial coverage of positive anomalies (figure 5.4(d)).

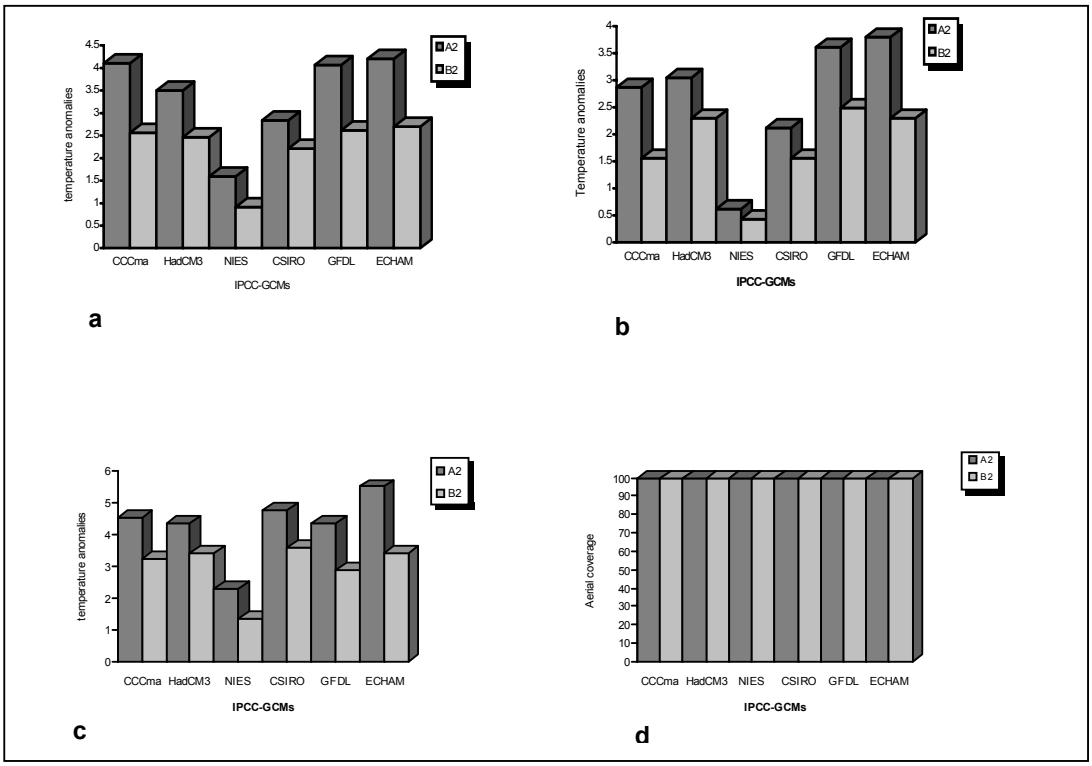

Figure 5.4: Spatially averaged near-surface temperature (^{o}C) projections for July 2080s for the A2 and B2 SRES scenarios over the Eritrea domain. The graphs denote spatial (a) averages, (b) minimum, (c) maximum and (d) aerial coverage (%) of positive anomalies of near-surface temperatures.

5.4.1.2 AVERAGE RAINFALL PROJECTIONS

Precipitation rate projections in mm.day^{-1} for the 2080s as simulated by the six IPCC GCMs with the A2 and B2 SRES scenarios for July are illustrated in figures 5.5 and 5.6, respectively. Again, due to the coarse grid resolution no detail is available for Eritrea.

Unlike the consistent above-baseline near-surface temperature projections, mixed signals of above and below baseline rainfall appear in the GCM projections. Note

that according to most IPCC GCMs large parts may expect drier condition comparing to present climate. The CSIRO and CCCma GCMs, in particular, simulated a rainfall decrease over most of the region under both SRES scenarios. According to grid boxes that cover Eritrea the majority of IPCC GCMs indicate a general increase of rainfall over Eritrea. That is in contrast to the bias towards drier conditions over the complete domain. In this regard, the HadCM3, ECHAM4, GFDL99 and NIES99 simulated wetter condition for Eritrea, while the remaining two GCMs (CCCma and CSIRO) simulated relatively drier conditions in comparison to the present climate. Despite of the wetter conditions projected by the majority of IPCC GCMs, mixed signal occur that imply a lack of inter model consistency amongst the IPCC GCMs as illustrated in figure 5.7. This poses uncertainty on what to expect in rainfall totals over the coming decades.

The spatial averaged GCM rainfall departures for Eritrea are in the order of +0.4 mm. day^{-1} and +0.5 $mm.day^{-1}$ for the A2 and B2 SRES scenarios, respectively (figure 5.7(a)). The spatially averaged, minimum (figure 5.7(b)) and maximum (figure 5.7(c)) values for Eritrea are in the range of –0.6 $mm.day^{-1}$ and +1.6 $mm.day^{-1}$ for the A2, and –0.5 mm day^{-1} and +1.8 mm day^{-1} for the B2 SRES scenarios.

Generally, the analysis shows that one might expect an increase in rainfall for July in the 2080s for the Eritrea, with mixed signals where the CSIRO GCM simulated the smallest percentage of wetter grid boxes (17.6%) while the HadCM3 and NIES99 with 100% wetter grid boxes (figure 5.7(d)).

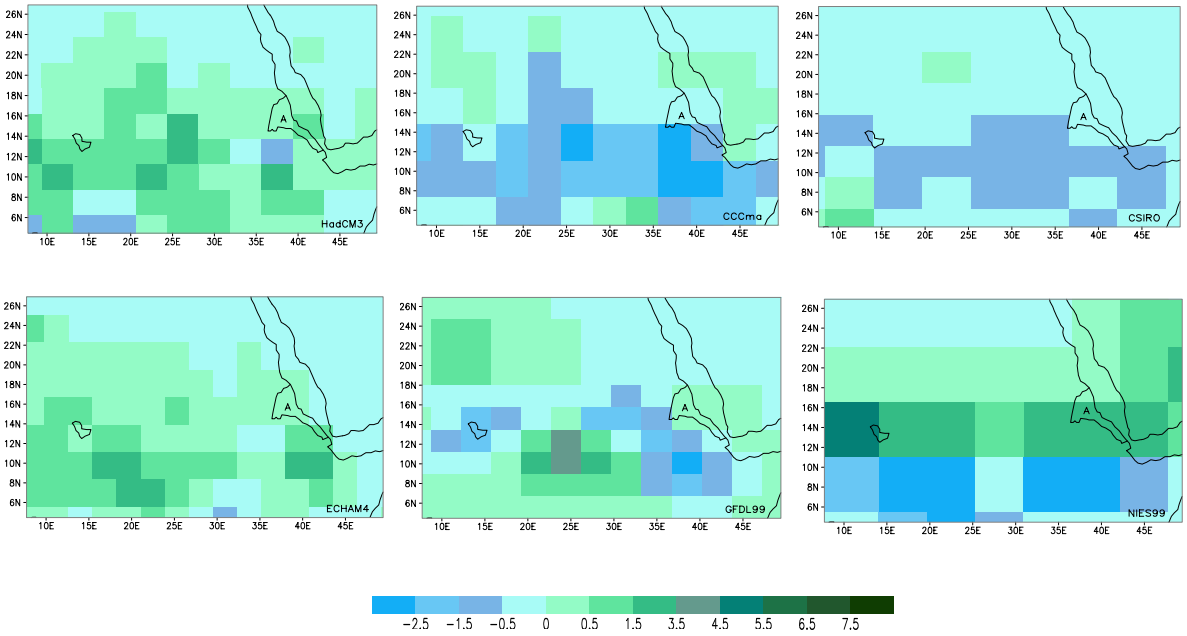

Figure 5.5: July rainfall (mm.day^{-1}) projections for the 2080s relative to 1961-91 for the six IPCC GCMs (indicated in the right bottom of each plot) for A2 SRES scenario. Eritrea is indicated in letter "A".

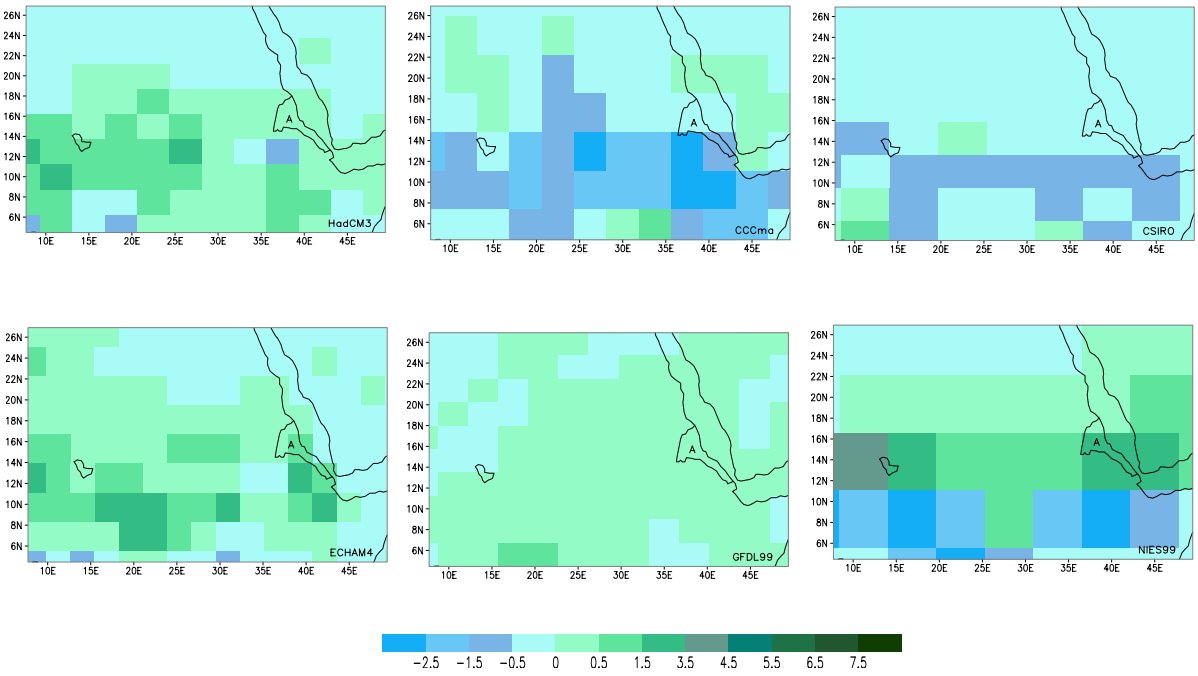

Figure 5.6: As figure 5.5 but for the B2 SRES scenario

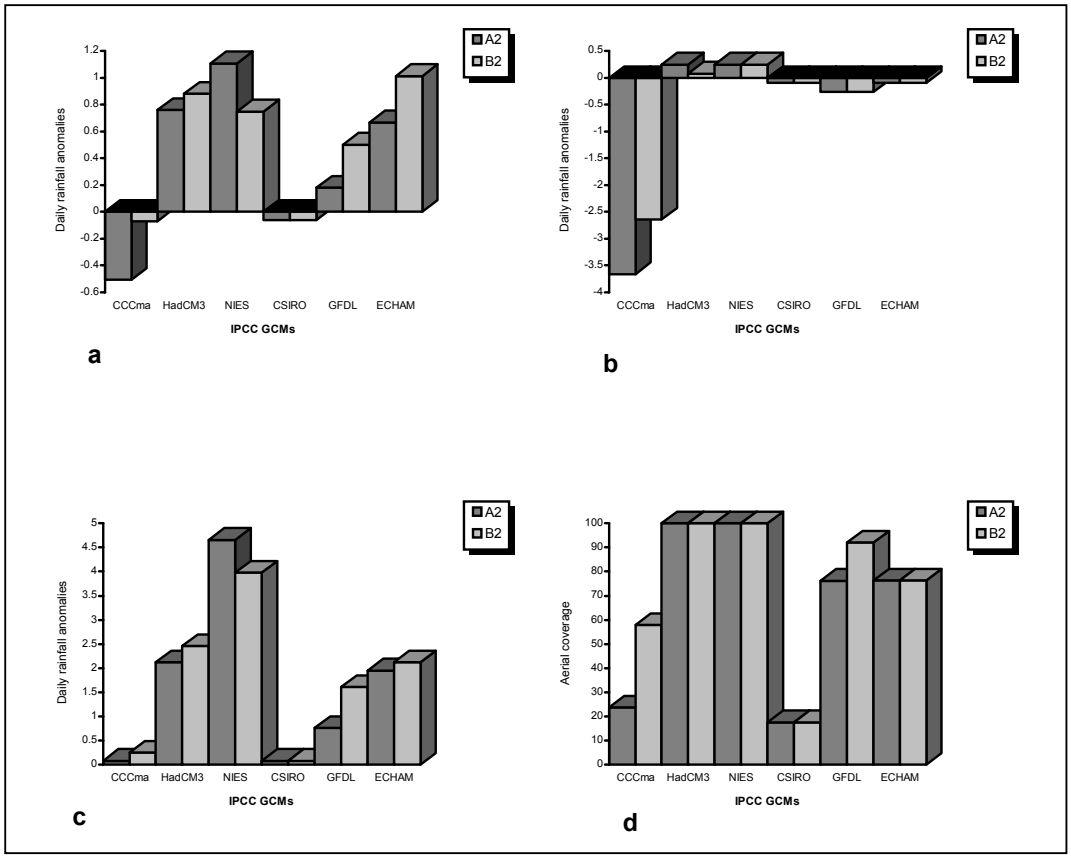

Figure 5.7: Spatially averaged rainfall (mm day^{-1}) projections for July 2080s for the A2 and B2 SRES scenarios over the Eritrean domain. The graphs denote spatial (a) averages, (b) minimum, (c) maximum and (d) aerial coverage (%) of positive anomalies of rainfall.

5.4.2 IPCC SIMULATED CLIMATE CHANGE SCENARIOS FOR JANUARY

5.4.2.1 AVERAGE NEAR-SURFACE TEMPERATURE PROJECTIONS

A2 and B2 SRES scenarios GCM projections of near-surface temperature for the 2080s as simulated by the six IPCC GCMs over the domain in figure 4.4 for January are illustrated in figures 5.8 and 5.9, respectively.

In agreement with the July simulations, above baseline near-surface temperature departures are generated for the 2080s. The spatial distribution of the projections, however, is less uniform than for July. When the whole domain is considered, the

GCMs captured locations of maximum near-surface temperature enhancement differently. The CCCma, for instance, simulated maximum near-surface temperature values over the western section, the ECHAM4 and GFDL99 over the southern section, while the CSIRO produce maximum values over the northern section of the domain. Nevertheless, apart from differences in magnitude, there is a plausible spatial agreement between all GCM simulations forced by the two SRES scenarios (A2 and B2).

The possibility that one might expect warmer January near-surface temperatures over Eritrea in the 2080s are simulated for both the A2 and B2 SRES scenarios (figure 5.10). Interesting to note is that there appear to be a stronger inter model consistency in average near-surface temperature projections compared to the July simulations (figure 5.4(a)) because of the comparable signal captured by NIES99 i.e., 4.42^{o}C (A2 SRES scenario) and 3.38^{o}C (B2 SRES scenario).

The spatial averaged GCM near-surface temperature departures for Eritrea are in the order of +3.9^{o}C and +3.1^{o}C for the A2 and B2 SRES scenarios, respectively (figure 5.10(a)). The spatially averaged minimum (figure 5.10(b)) and maximum (figure 5.10(c)) values for Eritrea are in the range of +3.4^{o}C and +4.7^{o}C for the A2, and +2.6^{o}C and +3.8^{o}C for the B2 SRES scenarios.

In general, the analysis concludes that one might expect an increase in the trend of January near-surface temperatures towards the 2080s over the Eritrea sub domain with a 100% spatial coverage of positive anomalies (figure 5.10(d)).

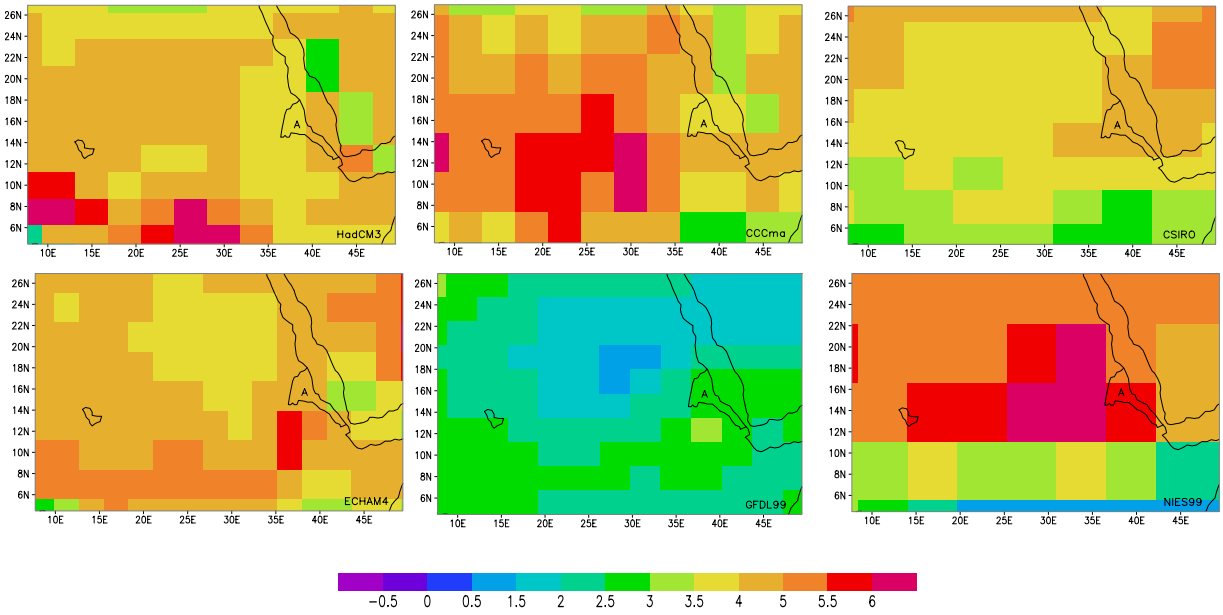

Figure 5.8: January near-surface temperature (°C) projections for the 2080s relative to 1961-90 for the six IPCC GCMs (indicated in the right bottom of each plot) for the A2 SRES scenario. Eritrea is indicated in letter "A".

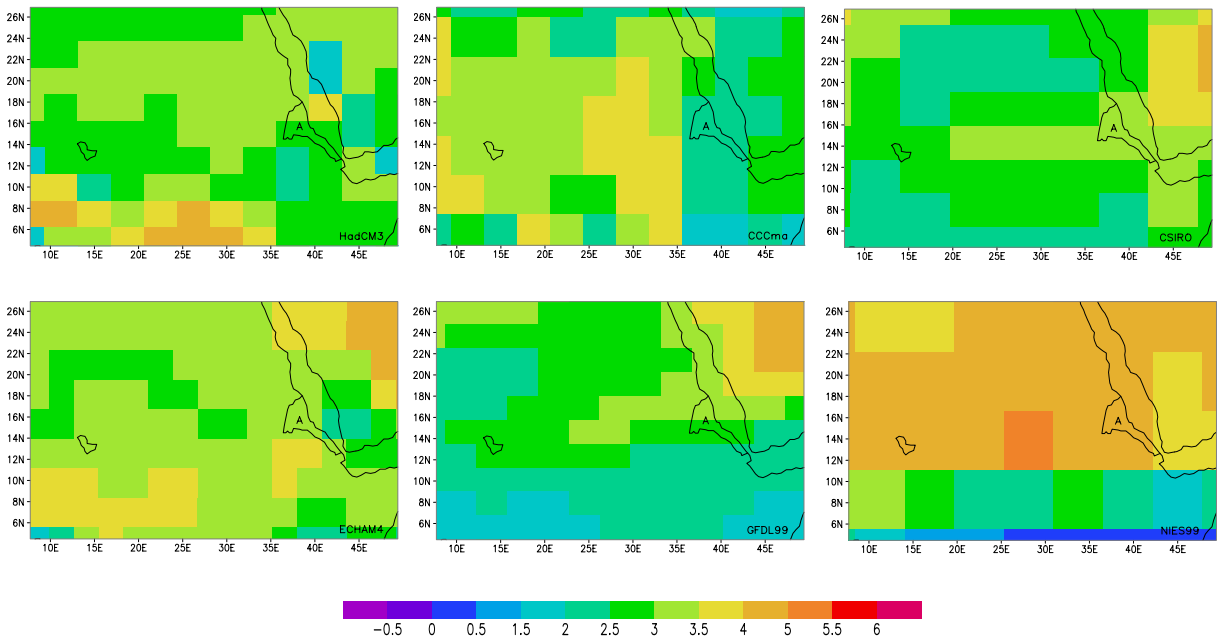

Figure 5.9: As figure 5.8 but for the B2 SRES scenario

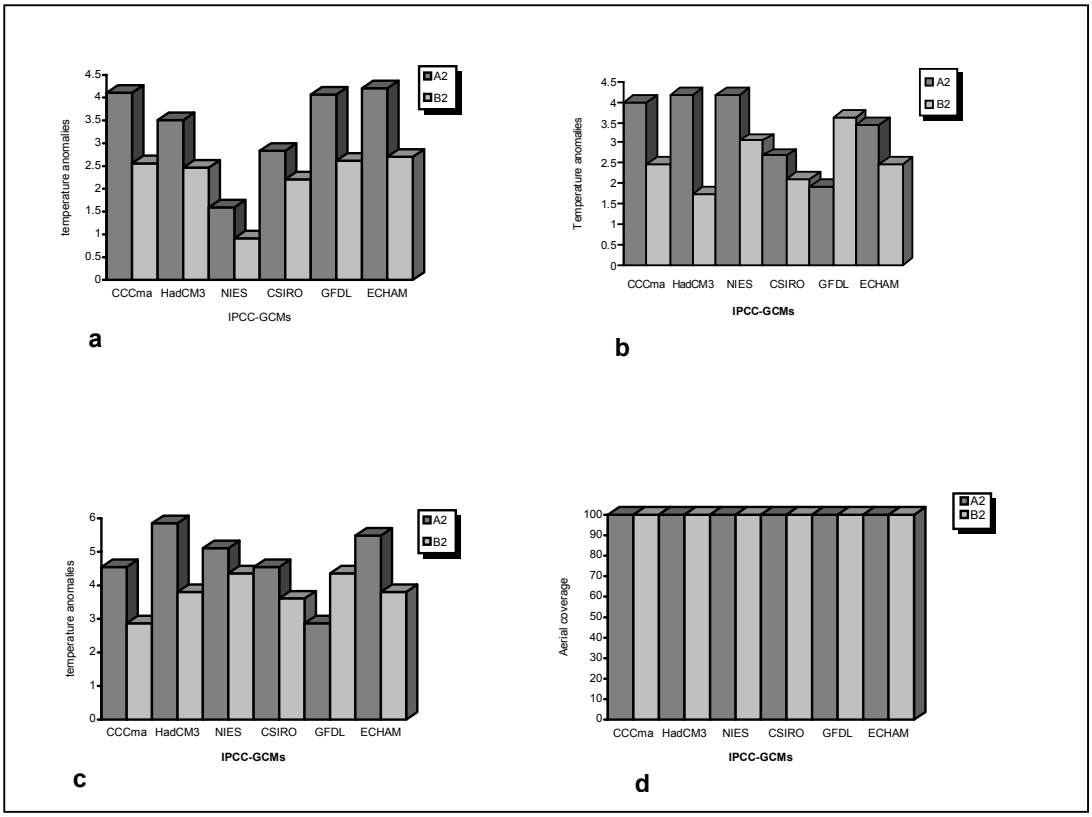

Figure 5.10: Spatially averaged near-surface temperature (^{o}C) projections for January 2080s for the A2 and B2 SRES scenarios over the Eritrea domain. The graphs denote spatial (a) averages, (b) minimum, (c) maximum and (d) aerial coverage (%) of positive anomalies of near-surface temperatures.

5.4.2.2 AVERAGE RAINFALL PROJECTIONS

Precipitation rate projections in mm.day^{-1} for the 2080s as simulated by of the six IPCC GCMs with the A2 and B2 SRES scenarios for January are illustrated in figures 5.11 and 5.12, respectively.

The projected January rainfall departures should be viewed from the perspective of observed regional rainfall behavior. During January, most of the region experiences dry condition (Boreal winter) and thus any projected changes by the IPCC GCMs on non-rainfall parts can only be a fluke. Some parts of the domain, however, receives rainfall associated with tropical circulation (the southern

extreme) or with regional disturbances (Ethiopia and eastern section of Eritrea) and thus, the analysis only focus on these regions.

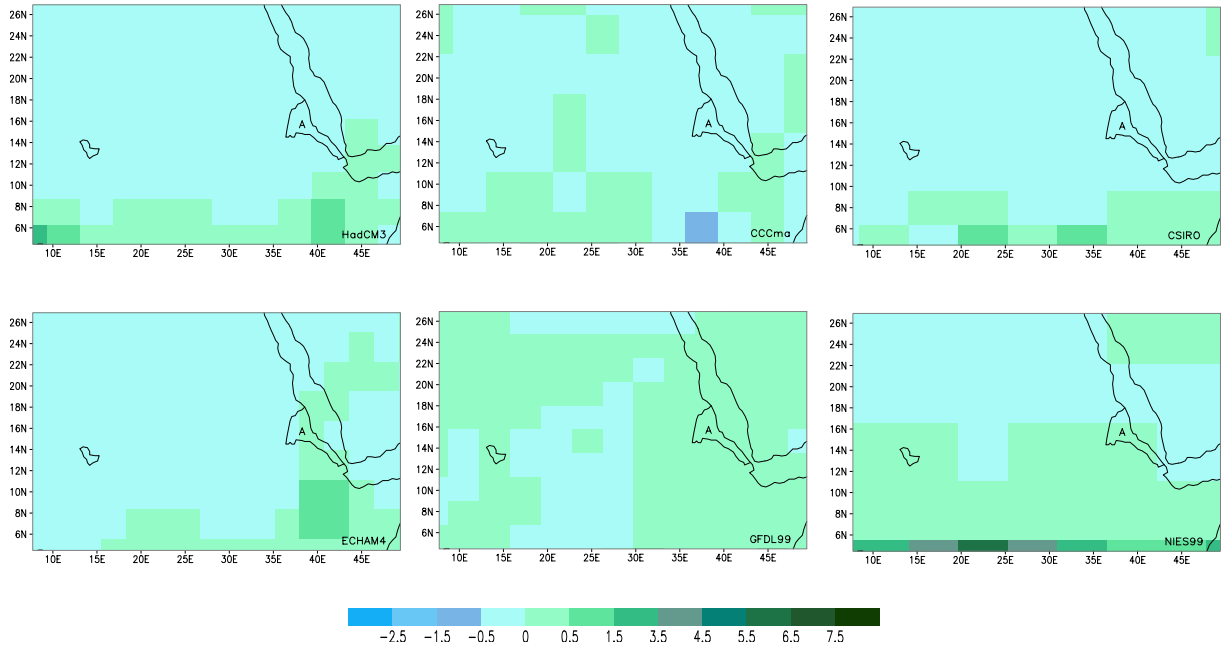

Figure 5.11: January rainfall (mm.day^{-1}) projections for the 2080s relative to 1961-91 for the six IPCC GCMs (indicated in the right bottom of each plot) for A2 SRES scenario. Eritrea is indicated in letter "A".

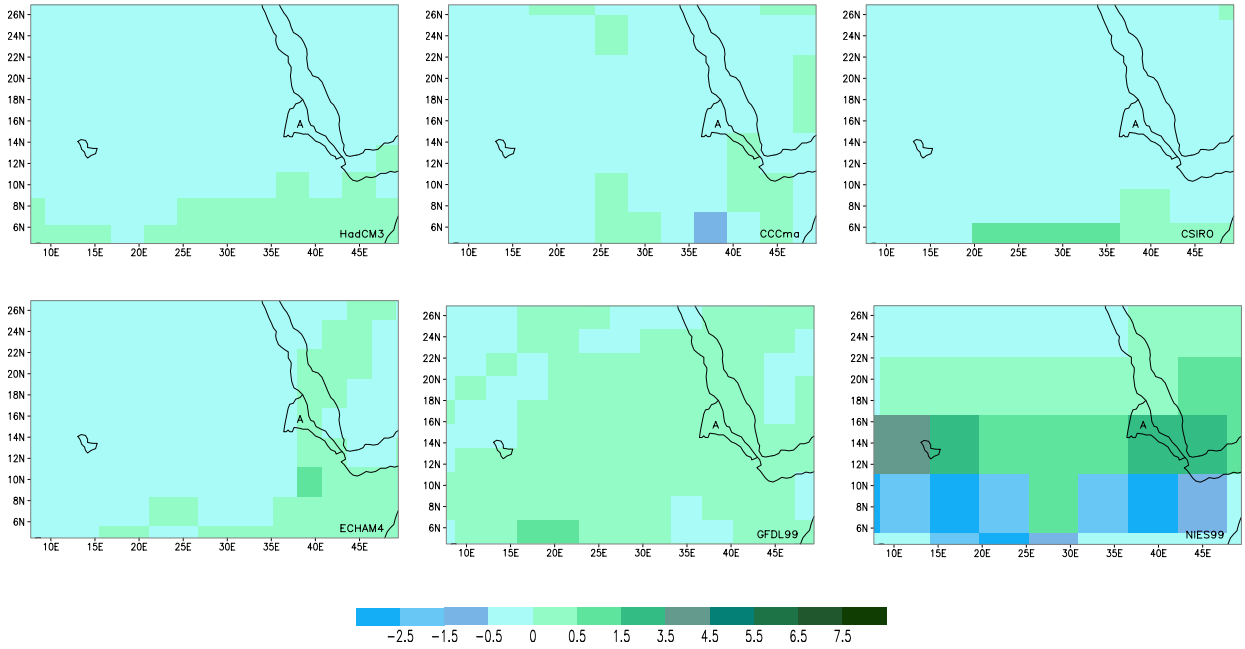

Figure 5.12: As figure 5.11 but for the B2 SRES scenario

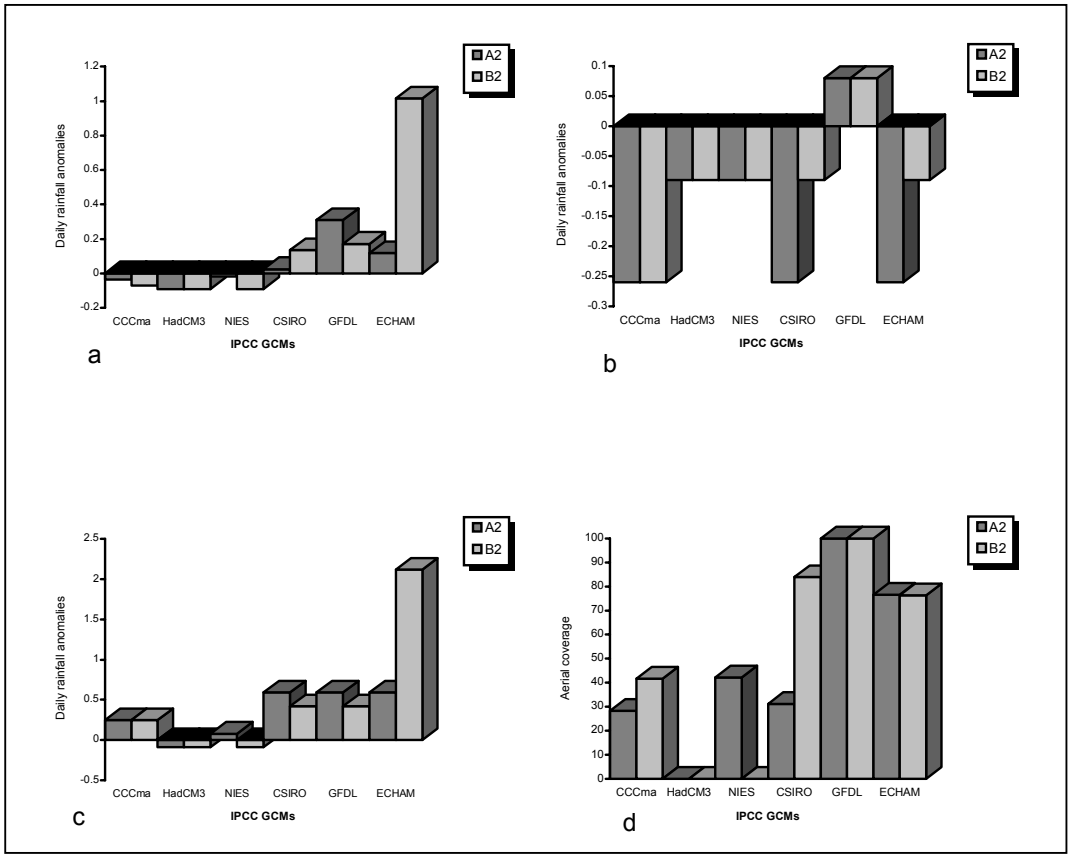

Figure 5.13: Spatially averaged rainfall (mm day^{-1}) projections for January 2080s for the A2 and B2 SRES scenarios over the Eritrean domain. The graphs denote spatial (a) averages, (b) minimum, (c) maximum and (d) aerial coverage (%) of positive anomalies of rainfall.

Similar to the July climate projections, the January rainfall projections are also associated with a great extent of uncertainty. This is again attributed to mixed signals of projected rainfall distribution amongst IPCC GCM simulations. The majority of GCMs (ECHAM4, NIES99, CSIRO and CCCma) show an increase in rainfall for both SRES scenarios. The GFDL99 simulated wetter conditions for the B2 SRES scenario, although a decrease in rainfall appear over the southwestern section of the domain for the A2 SRESS scenario. The HadCM3 simulated drier conditions over most of the domain for both the A2 and B2 SRES scenarios.

January precipitation projections for the 2080s for the considered scenarios over the Eritrea sub domain is regarded as uncertain since most of area under investigation is located in the summer rainfall region. For this reason, the January (presently dry winter) grid box values should be scrutinized with caution when constructing the histograms in figure 5.13.